arXiv:1702.05135v1 [cond-mat.str-el] 16 Feb 2017

[1]

Driven dissipative dynamics and topology of quantum impurity systems

Karyn Le Hur[1], Loïc Henriet[2], Loïc Herviou[1,3], Kirill Plekhanov[4,1], Alexandru Petrescu[5], Tal Goren[1], Marco Schiro[6], Christophe Mora[3], Peter P. Orth[7]

[1] *Centre de Physique Théorique, Ecole Polytechnique, CNRS, Université Paris-Saclay, 91128 Palaiseau Cedex France*
[2] *ICFO-Institut de Ciencies Fotoniques, The Barcelona Institute of Science and Technology, 08860 Castelldefels (Barcelona), Spain*
[3] *Laboratoire Pierre Aigrin, Ecole Normale Supérieure-PSL Research University, CNRS, Université Pierre et Marie Curie Sorbonne Universités, Université Paris-Sorbonne Paris Cité, 24 rue Lhomond 75231 Paris Cedex 05 France*
[4] *LPTMS, CNRS, Univ. Paris-Sud, Université Paris-Saclay, 91405 Orsay, France*
[5] *Department of Electrical Engineering, Princeton University, Princeton, New Jersey, 08544*
[6] *Institut de Physique Théorique, Université Paris Saclay, CNRS, CEA, F-91191 Gif-sur-Yvette, France*
[7] *Department of Physics and Astronomy, Iowa State University, Ames, Iowa 50011, USA*

Abstract

Studying quantitatively the real time dynamics of quantum materials can be challenging. Here, we address dissipative and driven quantum impurities such as spin-1/2 particles. Integrating over the environmental degrees of freedom produces entropy, decoherence and disorder effects. At low temperatures, spin-bath entanglement and memory effects of a non-Markovian bath result in intricate spin dynamics that we describe in analogy to classical systems coupled to stochastic forces or fields and random walks. A paradigmatic example of environment is a one-dimensional ensemble of harmonic oscillators (boson bath or Luttinger liquid) which can give rise to a plethora of rich phenomena such as dynamical Coulomb blockade, quantum phase transitions due to dissipation-induced localization, Kondo physics and Quantum Brownian Motion. At the same time, such an environment can be seen as a transmission line transporting input and output microwave light signals. In this article, we present our efforts to describe quantitatively the stochastic aspect of such quantum trajectories in time, the dissipation induced by the environment, as well as dynamical and topological effects imposed by external time-dependent potentials (such as AC perturbations or Floquet perturbations periodic in time, light-matter coupling and Ramsey interferometry). To be more specific, we aim to describe unified concepts related to (i) an effectively classical description of the reduced spin dynamics using Bloch equations including stochastic fields; (ii) a Boltzmann-Gibbs thermalized formulation with an effective temperature to characterize the entangled steady state of the spin; (iii) the topology of a dissipative spin-1/2 particle on the Bloch sphere with driven Floquet systems. Extensions to an ensemble of spins will be addressed leading to synchronization phenomena and stochastic mean-field dynamics. Then, we introduce quantum simulators in mesoscopic systems, circuit quantum electrodynamics and ultra-cold atoms to describe other aspects of driven dissipative quantum dynamics and topology in relation with experiments.

Keywords: Dissipative and Driven Quantum Systems, Stochastic Spin Dynamics and Bloch Equations, Effective Boltzmann-Gibbs Description and Thermalization, Stochastic Mean-Field Theory, Topology and Floquet Systems, Kondo Physics, Disorder and Quantum Brownian Motion, Berezinskii-Kosterlitz-Thouless and Mott-Superfluid Transition, Light-Matter and Hybrid Systems, Quantum Materials and Quantum State Engineering

1. French Title: Dynamique Dissipative, Topologie et Simulateurs Quantiques

1. Introduction

1.1. Generalities

A physical system or quantum material composed of many particles is often difficult to describe quantitatively, even numerically. A good starting point to reach a qualitative (and often even quantitative) understanding of a many-body system is therefore to take a local point of view and focus on a zero-dimensional quantum impurity system that is coupled to infinitely many degrees of freedom in its environment. Simple exemples are quantum impurities, spin-1/2 and double-well systems (see Fig. 1). Typical examples of this point of view are the Brownian motion and the Caldeira-Leggett model [1, 2]. Other important models concern a spin-1/2 particle coupled to a fermionic bath which is related to the Kondo effect in metals [3, 4, 5, 6], or a spin-1/2 particle coupled to a bosonic quadratic environment [7, 8, 9]. An important step made by Feynman and Vernon in 1963 was to suggest an Hamiltonian description of an environment in terms of a bath of harmonic oscillators [10]. This reasoning has also produced some progress on the development of methods such as the dynamical mean-field theory [11]. Interpolating between the high and low-temperature regime also allows to characterize the crossover between statistical physics (high temperature, where the environment essentially fixes an external temperature and produces decoherence) and the quantum physics (low temperature, characterized by the emergence of quantum entanglement and quantum coherence). These models, which are exactly solvable analytically or numerically [5, 12, 13], offer a plethora of unusual phenomena such as dissipation-induced quantum phase transitions and dynamical crossovers at zero temperature [14]. These models have attracted attention on their own due to novel applications in quantum biology [15], quantum optics and quantum information [16, 17]. We note some analogy between the Jaynes-Cummings model in cavity and circuit Quantum Electrodynamics (cQED), quantum fluids of light [18, 19, 20, 21, 22, 23, 24] and Bose-Hubbard physics in ultra-cold atoms [25].

In this article, we describe quantitatively the interplay between dissipation mediated by an environment and dynamical effects imposed by external time-dependent signals such as Floquet perturbations which are periodic in time. This class of problems refers to dissipative, driven and open quantum systems [26, 27, 28], which may also find applications to realize and probe topological phases [29, 30, 31]. Then, we present modern Feynman quantum simulators. A typical example of environment is a one-dimensional transmission line [32, 33], which can mimic a circuit-QED array [19, 22], a Luttinger liquid [34, 35], a Josephson junction array [36, 37] or a one-dimensional Bose-Einstein condensate (BEC)[38, 39, 40, 41], and can be described as an ensemble of harmonic oscillators. This environment is referred to as a ohmic environment. Even in the case of a simple tunnel junction, the effect of such a dissipative environment modeling Johnson-Nyquist noise from the external circuit [42], can deeply affect the I-V characteristics, as shown in Fig. 1, and produce dynamical Coulomb blockade physics at large resistances [43, 44]. This is also related to the Kane-Fisher tunnel barrier model [45, 46], and more generally to disorder physics in Luttinger liquids [47]. Dissipation effects at quantum phase transitions and dissipation-induced quantum phase transitions have already been observed in superconducting systems [48], cQED systems [49], and one-dimensional environments [43, 50]. Efforts to simulate environments with quite large impedances have also been realized in the context of the ohmic spin-boson model [51], and it is important to mention that time-dependent Ramsey interferometry in tunnel junctions could probe dynamical Coulomb blockade physics in time at weak resistances through current noise measurements [52]. Ramsey interferometry has been recently proposed theoretically for ensembles of fields [53] and spins [54], and generalized and applied in the context of topological phases in ultra-cold atoms [55]. A relation between two-time correlators, Loschmidt echo and Ramsey interferometry has also been studied in Luttinger liquids [56, 57].

Integrating out the degrees of freedom of an ohmic (Gaussian) type environment produces unusual memory effects in time in the low-temperature regime [10, 58, 59]. In the context of quantum spin trajectories on the Poincaré-Bloch sphere, this has led to the notion of interacting quantum blips and sojourns in time [8, 9], producing randomness on a path to go from a given point to another point. This disorder in time induces novel many-body physics, related to Kondo, Ising physics and localization transitions [7, 60]. We note that a crystal in time has been recently observed experimentally [61, 62]. For the ohmic spin-boson model, the emergent quantum phase transition is of Berezinskii-Kosterlitz-Thouless type as in the two-dimensional XY model, and is associated with the production of defects in the time domain (here corresponding to spin flips of the spin-1/2 particle). This engenders a jump of the spin magnetization and the spin remains localized by the environment in one of the two wells, or one of the two spin polarizations [60, 63, 64]. This analogy can be understood from renormalization group arguments

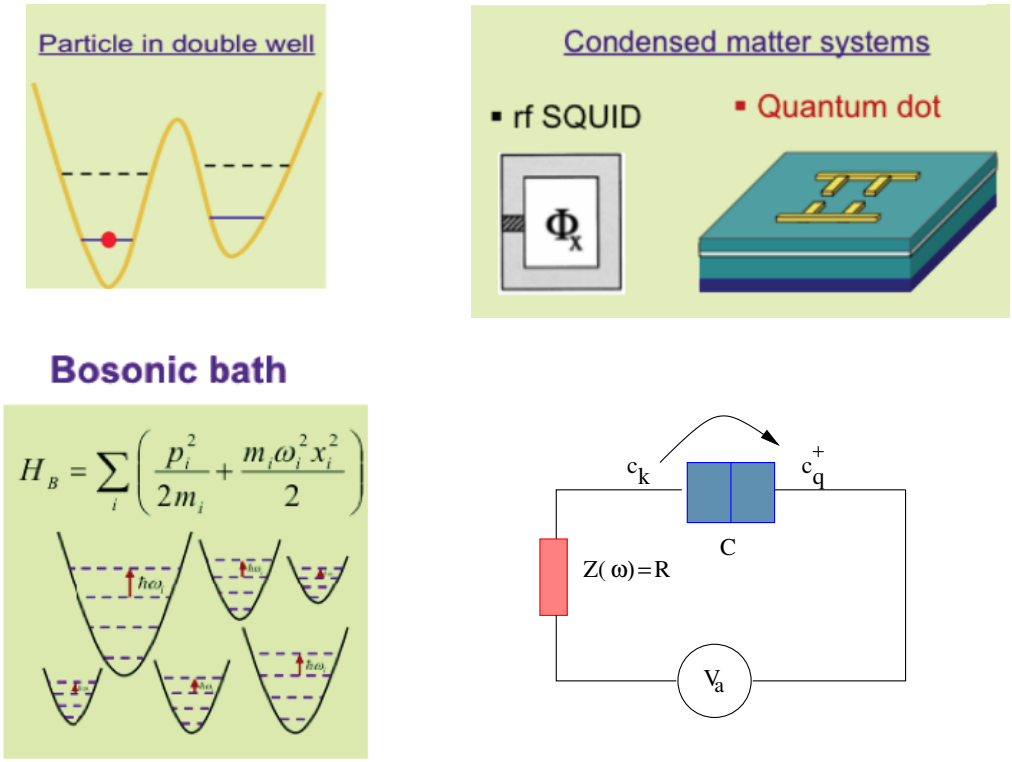

FIGURE 1 : Examples of Macroscopic Systems modeled as an effective two-level system or spin-1/2 particle, in relation with Sec. 3. A double-well system built in optical lattices for example, with one extra particle in the two wells, will be used as a quantum microscope to probe the superfluid-Mott transition in a ladder system in Sec. 3.4 (in ultra-cold atoms, energy scales can reach nano-Kelvins). Two-energy levels of an atomic energy spectrum can now be realized artificially with superconducting qubits or quantum dots (with much smaller energy scales $\sim Kelvin$ and acting in the microwave limit of light) will allow us to realize novel many-body physics in contact with a macroscopic environment ; see Secs. 3.1-3.3. Applications of an external magnetic flux Φ also leads to novel interferometry or novel physics, see Sec. 3.4 (Meissner effect, vortex phases, quantum Hall and Laughlin physics). Magnetic fluxes can also be generated artificially through time-dependent Floquet perturbations, periodic in time, or through interactions in the system. Concerning the role of dissipation, a typical example is an ohmic environment which can be viewed as a bath of harmonic oscillators, Luttinger liquid, or a resistance (impedance at zero frequency) in an external circuit which produces non-linear I-V characteristics in transport.

[4]. Solving real-time dynamics is often difficult and requires the development of methods, even in a mean-field picture. Exactly solvable limits exist, for example related to exact mappings between bosons and fermions in one dimension, at and around the Toulouse limit [65, 66, 67]. In addition, this is directly related to experimental efforts in quantum circuits, where single trajectories can now be tracked on the Bloch sphere [68, 262]. Decoupling the interactions in time is possible through the introduction of Hubbard-Stratonovich variables in the Feynman path integral sense. Then, one reaches a quantum stochastic theory with Hubbard-Stratonovich fields as stochastic classical variables [70, 71, 72, 73, 74, 75, 76]. Averaging over these noisy fields, one can follow the reduced density matrix of the system in time. This way of thinking has led to the development of local type stochastic Schrödinger equation approaches [70, 71, 72, 73, 74, 75, 76]. Inspired by these earlier works, we have developed and applied this concept to driven and dissipative Landau-Zener models [77], Rabi models and dissipative spin systems [78, 79, 80], and addressed various classes of time-dependent situations. By analogy to developments in the context of disordered problems [81], driven light-matter systems and coupled spin systems require more than one stochastic field to treat the real-time dynamics rigorously [78, 79, 80].

It is important to mention the development of numerous numerical methods to treat driven and open systems,

such as stochastic wave-function approaches [82, 83, 84, 85], Numerical Renormalization Group (NRG) approaches [86, 87, 88, 89, 90], Quantum Monte Carlo approaches [91, 92, 93, 94], master equations [95, 96], Matrix Product States methods and Cluster Mean-Field Approaches [97, 98, 99, 100], Combinations of variational matrix product states and coherent state expansions [101]. Stochastic or Monte-Carlo approaches have also been developed further for quantum lattice systems at equilibrium [47, 81, 102, 103, 104, 105, 106, 108, 109] and for driven and open systems [110, 111]. Below, we will also apply bosonization methods [34, 35] that can be combined with Keldysh methods to address non-equilibrium transport problems [28].

1.2. Goals of the Paper

Here, we summarize the main objectives of this paper. We review our current efforts in the field and also show some novel results and applications.

First, we present a simple analogy between classical Bloch equations in relation with the Nuclear Magnetic Resonance (NMR) and the time-evolution of the spin observables in the quantum limit of the ohmic spin-boson model, obtained with the stochastic Schrödinger equation approach [77]. We also summarize the relation with the non-interacting blip approximation [8, 9]. Following Ref. [112], we show how we can define an effective temperature T_{eff} for the reduced system entangled with the environment in the quantum limit [113, 114] by making an analogy with an effective Boltzmann-Gibbs description in the statistical sense. We will use this concept of effective temperature to connect with the coherent-incoherent quantum spin dynamics crossover and population inversion. Such an inversion of population can lead to negative (absolute) temperatures, as observed in ultra-cold atoms [115]. Then, we address topology of a driven and dissipative spin-1/2 particle on the Bloch sphere, in relation with the Berry phase [117] and Chern number measurements [116, 118], current experiments in cQED systems [119, 120] and ultra-cold atoms [121, 122, 123]. It is also important to mention current experiments in quantum materials to access Berry phase informations [124, 125, 126]. The topology of the spin is measured by a bipartite measurement (north and south pole measurements of spin magnetization on the sphere). By changing the polar angle linearly in time and increasing the speed of the protocol, we report a quantum dynamo effect where rotating the spin (or artificial qubit) on the sphere produces 'artificial photons' in the environment compensating the applied magnetic field [80]. We describe this effect by a toy model with a one-mode environment, making an analogy with the quantum Dicke model [127, 128]. We use this view point to connect with dissipative and driven spin chains with long-range forces [39, 40, 78, 130, 131] which find various realizations (simulators) [132, 133, 134, 135]. Then, we show how an environment can be used to induce long-time synchronization of two spins [78, 90, 137]. We also note that synchronization mechanisms have been observed in ultra-cold atoms [138], and unify Josephson junction physics or Bose-Hubbard models and Neural synchronization, through the Kuramoto model [139, 140].

The anti-symmetrized spin-spin correlation function in time is also deeply related to the fluctuation-dissipation theorem for the dynamical spin susceptibility through the Korringa-Shiba relation [141, 142] and the emergent Fermi liquid ground state [6, 143]. We show applications of this relation in the spin-boson and Kondo models, and more precisely in the context of Kondo resonance of light [144, 145], AC driven quantum RC circuits [146, 147], and the physics of hybrid systems comprising mesoscopic electron systems and a cQED environment [148, 149, 150]. This research is directly related to recent experimental developments in driven mesoscopic systems and hybrid light-matter systems [146, 151, 152, 153]. We propose an analogy of the Friedel's phase in relation with the input-output theory in the AC regime [154].

Then, we study several aspects of the quantum Brownian motion [155] in relation with Kondo and quantum impurity physics. More precisely, we address multi-channel Kondo realizations [156] of topological mesoscopic boxes [157, 158, 159, 160, 161] and we analyze the feedback of the non-linear transport through a mesoscopic quantum dot on the quantum electrodynamics of a cavity [148]. From fluctuation-dissipation relations, using the Schwinger-Keldysh approach, one can build a classical Langevin equation and derive an effective temperature T_{eff} for the cavity beyond the equilibrium limit. These hybrid systems have also attracted some attention in the context of nano machines and thermoelectricity [162], and novel platforms to probe Kondo physics with light [152, 153]. We also note the recent realizations of two-channel Kondo physics in mesoscopic systems [163, 164], inspired by theory [165, 166]. Finally, we simulate a quantum microscope as a spin-1/2 particle [167] to probe the superfluid-Mott transition in a ladder system [168, 169, 170, 171] and show that ladder systems can be useful to probe novel phases with chiral currents [172, 173, 174], in relation with Floquet theory [175, 176] and

spin-boson systems [177, 178]. Quantum microscopes have already been built in ultra-cold atoms [179, 180, 181] and similar experiments have been implemented with superconducting circuits [182].

2. Dynamics of Spins

2.1. General Arguments and Bloch equations

Let us start to study the dynamics of a spin-1/2 particle subject to dissipation in an applied field $\mathbf{H}_{appl}$ along the z direction. The state of the system at any time t can be specified uniquely by giving expectation values $\langle\sigma_i(t)\rangle$ of the Pauli operators (spin components) at this time. Omitting the argument t, the (reduced) density matrix of the spin reads

$$\hat{\rho} = \begin{pmatrix} \frac{1}{2}(1+\langle\sigma_z\rangle) & \frac{1}{2}(\langle\sigma_x\rangle + i\langle\sigma_y\rangle) \\ \frac{1}{2}(\langle\sigma_x\rangle - i\langle\sigma_y\rangle) & \frac{1}{2}(1-\langle\sigma_z\rangle) \end{pmatrix}.$$

A pure state must satisfy $\hat{\rho}^2 = \hat{\rho}$ implying $\langle\sigma_x\rangle^2 + \langle\sigma_y\rangle^2 + \langle\sigma_z\rangle^2 = 1$. In this case, the state is an eigenstate of $\mathbf{n}\cdot\sigma$ where $\mathbf{n}$ is a unit vector; the spin points along $\mathbf{n}$.

If the spin-bath coupling is sufficiently weak, one expects the celebrated Bloch equations (which describe memoryless time-local induced relaxation and decoherence effects) to be valid, where $S_i = \langle\sigma_i\rangle/2$:

$$\begin{aligned} \frac{dS_z}{dt} &= -\frac{S_z - S_z^{(eq)}}{T_1} \\ \frac{d\mathbf{S}_\perp}{dt} &= \omega_0 \mathbf{z}\times\mathbf{S}_\perp - \mathbf{S}_\perp/T_2, \end{aligned} \tag{1}$$

where ω_0 is the Larmor frequency associated with the applied field $\mathbf{H}_{appl} = \omega_0\mathbf{z}$ (for simplicity, we have taken the gyromagnetic ratio equal to 1). Assuming thermal equilibrium, for the case of weak-coupling with the thermal bath leads to :

$$S_z^{eq} = \frac{1}{2}\tanh(\beta\omega_0/2). \tag{2}$$

In this expression, $\beta = 1/(k_B T)$. At zero temperature the spin is in the ground state and $S_z^{eq}(T=0) = 1/2$ while thermal fluctuations lead to $S_z^{eq} < 1/2$ when $T > 0$. Note that a population inversion refers to $S_z^{eq} < 0$ and corresponds effectively to a negative (absolute) temperature. This situation will occur below based on purely non-equilibrium dynamical protocols. The times T_1 and T_2 are the longitudinal and transverse spin relaxation times measured in NMR. A straightforward theory of T_1 and T_2 can be obtained by writing down the exact equation of motion

$$\frac{d\mathbf{S}}{dt} = \omega_0\mathbf{z}\times\mathbf{S} - \mathbf{S}\times\mathbf{H_{env}}, \tag{3}$$

where $\mathbf{H}_{env}$ is a Markovian (i.e. memoryless) stochastic magnetic field that captures the effect of the environment on the spin. Averaging over the stochastic fluctuations of $\mathbf{H}_{env}$, assuming that the environment is unperturbed by the dynamics of the spin then leads to Eq. (1).

To reach Eq. (2), we have assumed the situation where $\mathbf{H}_{env}$ has only a component along the z direction, then the complete behavior of $\mathbf{S}(t)$ is determined by the spectral density $J(\omega)$ of the environment. The environmental fields are entirely along the z-direction. Let us start at time $t = 0$ with the spin polarized along (say) the x-direction. It is convenient to eliminate the effect of Larmor precession by going to a frame rotating with angular velocity ω_0 along the z-axis. Then, we define the complex quantity $S_x + iS_y = S_\perp e^{i\varphi}$ for any realization of the noise, its magnitude $|S_\perp|$ will remain constant (equal to $1/2$ according to the definitions) and the phase will precess as a result of the noisy environment, with a new operator $B(t)$ related to $\mathbf{H}_{env}$

$$\hbar\frac{d\varphi}{dt} = B(t) \rightarrow \varphi(t) = \int_0^t B(t')dt'/\hbar. \tag{4}$$

Assuming a Gaussian statistics for B (which is satisfied for an ensemble of harmonic oscillators) then

$$\langle \exp i \int_0^t B(t')dt' \rangle = \exp -\frac{1}{2} \int_0^t dt' \int_0^t dt'' \langle B(t')B(t'') \rangle. \tag{5}$$

For a Markovian environment, e.g. based on harmonic oscillators at high temperatures (where $\langle B(t')B(t'') \rangle \propto k_B T \delta(t'-t'')$), then the dominant behavior at long times t is

$$(S_x + iS_y)(t) \equiv \exp(-t/T_2), \tag{6}$$

where

$$T_2^{-1} = 2\pi \lim_{\omega \to 0} \coth(\beta\hbar\omega/2) J(\omega). \tag{7}$$

For the Johnson-Nyquist environment (ohmic bath) addressed in the the next sub-section, $J(\omega) = \eta\omega$ and thus for $\beta\hbar\omega \ll 1$

$$T_2^{-1} \sim \eta k_B T/\hbar. \tag{8}$$

Obviously, the environment produces decoherence on the off-diagonal elements of the spin reduced density matrix and the spin will relax to a thermal equilibrium state along z direction at very long times. This argument is very general and is valid for any form of environment, in fact.

Below, we explore and engineer the properties of an environment, in particular ohmic, beyond the weak-coupling regime producing novel entanglement and dephasing mechanisms. It is also convenient to introduce entanglement measures in this context such as the entanglement entropy between spin and environment $S = -\mathrm{Tr}(\hat{\rho} \log \hat{\rho})$ [113, 114]. To simplify the notations, we normalize the Planck constant $\hbar$ to unity.

2.2. Stochastic Point of View in the quantum limit, Disorder in time, and Effective Boltzmann-Gibbs Description

Now, let us address the quantum limit where $T_2 \to +\infty$ for the ohmic bath. Below, we show that since the bath is subject to zero-point fluctuations, this will still cause decoherence and entanglement. Even in the absence of thermal fluctuations at $T = 0$ the (small) spin-1/2 system is affected by the quantum fluctuations of the bath; we show that under certain conditions, spin observables can be re-interpreted as an effective thermal state with an effective temperature.

Let us consider the standard spin-boson Hamiltonian [8, 9] :

$$\hat{H} = \frac{\Delta\sigma_x}{2} + \frac{h_z\sigma_z}{2} + \frac{\sigma_z}{2} \sum_k \lambda_k (b_k^\dagger + b_k) + \sum_k \omega_k b_k^\dagger b_k. \tag{9}$$

The Ohmic spectral function is defined as $J(\omega) = \pi \sum_k \lambda_k^2 \delta(\omega - \omega_k) = 2\pi\alpha\omega e^{-\omega/\omega_c}$ such that the dimensionless friction (dissipation) coefficient is now defined as $\eta = 2\pi\alpha$. Below, we consider the situation where $\omega_c \gg \Delta$. One can absorb the spin-bath coupling by performing a rotation $U = \exp(i\varphi\sigma_z/2)$ with $\varphi = i\sum_k \frac{\lambda_k}{\omega_k}(b_k^\dagger - b_k)$. The spin observables then are completely absorbed in a redefinition of the spin components in the xy plane, $\sigma^+ \to \sigma^+ e^{i\varphi}$ and $\sigma^- \to \sigma^- e^{-i\varphi}$ [9]. This can be viewed as a polaron transformation. Increasing the coupling with the bath then produces fluctuations (disorder) in the phase φ. Note that the applied magnetic field Δ here is defined along the x-axis, and in this subsection $h_z = 0$ for $t > 0$; at time $t = 0$, the spin is in the $|\uparrow\rangle_z$ state.

2.2.1. Simple View of Stochasticity and Disorder or Random Walk in Time

Neglecting the feedback of the spin on the environment one can derive exact equations of motion for the spin based on exact Heisenberg equations of motion. This step has been summarized in the review [14] based on Ref. [59]. One obtains :

$$\frac{d}{dt} S_z = -\Delta^2 \cos(\pi\alpha) \int_0^t ds \exp(-Q_2(t-s)/\pi) S_z. \tag{10}$$

The prefactor is in accordance with Ref. [77], to make a connection with the stochastic approach. Here, we have neglected the feedback of the spin on the $\varphi(t)$ field correlation function leads to $\langle \cos[\varphi(t) - \varphi(s)] \rangle =$

$\exp(-Q_2(t-s)/\pi)$, and for a Ohmic bath $Q_2(t) = (\eta/2)\ln(1+\omega_c^2 t^2) + \eta\ln((1/k_B T t)\sinh(\pi k_B T t))$ [8, 9]. In the high-temperature limit one recovers an exponential suppression with $T_2^{-1} \sim \eta k_B T$. At zero temperature, we observe memory effects. In the absence of noise from the environment, the Q_2 function is equal to zero and one recovers the usual Rabi formula $d^2\langle\sigma_z\rangle/dt^2 = -\Delta^2\langle\sigma_z(t)\rangle$ meaning undamped oscillations between state $|\uparrow\rangle_z$ to $|\downarrow\rangle_z$ with a frequency Δ. The introduction of the environment produces damping similar to the harmonic oscillator. There is also a shift of the frequency of the oscillations and one can extract the quality factor through Laplace transform, the ratio of the renormalized frequency Ω versus the damping parameter γ, such that $\langle\sigma_z(t)\rangle \sim \exp(-\gamma t)\cos(\Omega t)$ [8, 9] :

$$\frac{\Omega}{\gamma} = \cot\frac{\pi\alpha}{2(1-\alpha)}. \tag{11}$$

The frequency and the damping rates are both proportional to the renormalized transverse field $\Delta_r = \Delta(\Delta/\omega_c)^{\alpha/1-\alpha}$ [8, 9]. The renormalized transverse field can also understood from the transformation $\sigma^+ \to \sigma^+ e^{i\varphi}$; this leads to $\Delta_r = \Delta\langle e^{i\varphi}\rangle$ where the average here is taken over the ground state of harmonic oscillators ($\langle e^{i\varphi}\rangle = e^{-\langle\varphi^2\rangle/2}$ and summing over modes from frequencies of the order of Δ to frequencies of the order of ω_c [8]). At the point $\alpha = 1/2$, which corresponds to the Toulouse limit [65], we observe that the Rabi oscillations disappear, which has been confirmed [8] by a free fermion resonant level mapping [66]. This quality factor has also been obtained from the non-interacting-blip approximation (NIBA) [8, 9].

It is important to note that, without assuming a separable state between spin and environment, Eq. (10) turns into :

$$\langle\dot{\sigma}_z(t)\rangle = -\Delta^2\cos(\pi\alpha)\int_0^t ds\langle\cos(\varphi(t)-\varphi(s))\sigma_z(s)\rangle. \tag{12}$$

In the regime beyond weak-coupling, in principle there exists correlations between the spin trajectories and the environment. At short times, these correlations are small. However, at long times or in non-equilibrium settings, these correlations become important showing the necessity to develop approaches to tackle these problems. By fixing the initial state and final state on the Bloch sphere, recent experiments have succeeded in tracking single-spin quantum trajectories [68]. In these noisy situations, one must average over the distribution of random fields and therefore also average on random paths (which act as a disorder in time) for a given spin trajectory. Remarkably, at equilibrium, one can write down the partition function of the spin in an exact manner by analogy to a Coulomb gas, following Anderson, Yuval and Hamman [58]. The disorder in time is well-known to produce a quantum phase transition at large couplings, by analogy to the antiferromagnetic-feromagnetic Kondo transition, where the spin becomes localized in a $|\uparrow\rangle_z$ or $|\downarrow\rangle_z$ state, by coupling to the bath for $\alpha \sim 1$. The phase transition is of Berezinskii-Kosterlitz-Thouless type and characterized by a jump in $\langle\sigma_z\rangle$ [60, 64, 113] by analogy to the superfluid stiffness in two-dimensional XY models. In addition, the expression for the reduced density matrix can also be written in real time as shown by Eq. (13). We also note current theoretical efforts to describe open random walks in terms of stochastic differential Lindblad equations [96].

At a general level, one can make an analogy with the classical Bloch equations [77]

$$\frac{d\mathbf{S}}{dt} = \mathbf{H}(t)\times\mathbf{S}(t). \tag{13}$$

The effective noisy magnetic field $\mathbf{H}(t)$ then lies in the x-y plane

$$\mathbf{H} = H_0(\cos\varphi(t), \sin\varphi(t), 0) = (H_x, H_y, H_z), \tag{14}$$

with $H_0 = \Delta\sqrt{\cos(\pi\alpha)}$. $\varphi(t)$ here represents a classical random field with identical correlation functions in time given by the Q_2 function. These equations can be reached exactly using a stochastic Schrödinger equation method by tracing out the (Gaussian) environment : the stochastic field φ is introduced as an Hubbard-Stratonovich field to decouple long-range correlations in time induced by the bath in the quantum limit. A detailed derivation of this equation can be found in Ref. [77] for the components y and z (for the x component, however certain assumptions do not hold). To have an intuition on these equations, the polaron transformation presented above helps to understand the effect of the bath as a random noisy phase (operator) associated with the S_x and S_y operators. The different spin components then satisfy $\dot{S}_x = H_y S_x$, $\dot{S}_y = -H_x S_z$ and $\dot{S}_y = H_x S_y - H_y S_x$. It is nevertheless

important to mention that in the blip and sojourn approach [8, 9], the initial and final boundary conditions must be taken with care. Starting from the earlier works in the literature [70, 71, 72, 73, 74], we have done several efforts in solving these stochastic equations beyond the decoupling between spin and bath.

First, we have checked that the method tends to confirm the quality factor in Eq. (11) (see Fig. 2), obtained from a weak-coupling expansion or a non-interacting blip approximation [8, 9], until $\alpha = 1/2$ [77]. This can be understood from the fact that the Toulouse point $\alpha = 1/2$ is special, the blips become non-interacting [8]. Beyond $\alpha = 1/2$, the method can suffer from convergence problems. The method then has been extended to Landau-Zener and Kibble-Zurek problems [77, 78]. It is important to note that in practice, the derivation of stochastic Schrödinger type equations can require more than one stochastic fields, as we have shown for example in the context of dissipative and driven light-matter systems [79] and for two dissipative coupled spins [78]. Spatial disorder problems in one dimension can also require more than one stochastic fields to solve the problem [81]. For dissipative coupled spins, results agree with previous results obtained with the numerical renormalization group [90] and with quantum Monte Carlo [91]. In addition, novel results have been obtained regarding synchronization of spins and the dynamics in the localized regime, as well as correlation functions between two spins [78].

2.2.2. Effective Boltzmann-Gibbs Thermal analogy

An analogy with a Boltzmann-Gibbs grand canonical ensemble can be formulated as follows. Let us replace the quantum bath by a thermal bath described by an effective temperature T_{eff}, such that $\beta_{eff} = 1/(k_B T_{eff})$, and weakly coupled to the spin, allowing for a statistical analogy. The spin-1/2 then would be described by the effective Hamiltonian $\hat{H} = \frac{1}{2}(\Delta^* \sigma_x + h_z^* \sigma_z)$ with eigenvalues are $E_\pm = \pm\sqrt{(\Delta^*)^2 + (h_z^*)^2}$. In this pseudo-equilibrium picture, the spin reduced density matrix is described by the two eigen-values $\lambda_\pm = \exp(-\beta_{eff} E_\pm)$. Following Ref. [112], then one can identify the eigenvalues of the spin reduced matrix in the spin-boson model in the quantum limit with the effective thermal Gibbs weights $\lambda_\pm$ leading to $T_{eff} = \sqrt{(h_z^*)^2 + (\Delta^*)^2}/\ln(\lambda_+/\lambda_-)$ [112]. From the spin-boson model at zero temperature, we also have $\lambda_\pm = 1/2(1 \mp p)$ where $p = \sqrt{\langle\sigma_x\rangle^2 + \langle\sigma_z\rangle^2}$ (here, $\langle\sigma_y\rangle = 0$) and the eigenvalues are calculated with the Hamiltonian in the quantum limit. In the weak-coupling limit of the spin-boson model, $\beta_{eff} = 1/(k_B T_{eff})$ tends to infinity as $\lambda_+ \to 0$. More precisely, the spin resides in its ground state with $p = 1$. Increasing the coupling with the quantum bath produces some uncertainty and mixed state for the spin-1/2 such that $0 \leq p < 1$. We also note that a similar steady-state Gibbs description has been introduced for driven mesoscopic systems [183, 184, 185, 186] and in one-dimensional quantum systems [187, 188, 189]. This way of reasoning has also led to the concept of entanglement spectrum in the field of many-body quantum entanglement ; when the sub-system is large enough one expects a universal effective temperature in the sub-system [190, 191]. It is also important to note applications of this concept in correlated quantum materials [192] and many-body localization [193, 194].

In Sec. 2.3, we apply this concept in relation with driven Floquet dynamics on the Bloch sphere and topology. In Sec. 3.3, we also make a connection with the quantum electrodynamics of a cavity field coupled to a mesoscopic system subject to a bias voltage.

At a general level, we note an analogy between thermal effects and increasing the coupling with environment in the quantum limit (see Fig. 2). Now, let us interpret the results of the Rabi dynamics at the Toulouse limit $\alpha = 1/2$ in terms of an effective steady-state thermodynamics. Remember, we apply the external field $H_{appl} = \Delta$ along the x direction. At the Toulouse limit $\alpha = 1/2$, we observe that similar to the high-temperature limit, at zero temperature $\langle\sigma_z(t)\rangle \sim \exp(-\gamma t)$, and we identify $\gamma = 1/T_2 = \Gamma$ where Γ can be interpreted as the width of an effective resonant level model $\Gamma \sim \Delta^2/\omega_c \sim \Delta_r$ [8, 9, 14]. Important quantitative results have also been obtained using the NRG [88] and analytical renormalization group methods [67]. T_2 traduces the typical time to form a Kondo-type resonance between the spin and the environment, and the spin will relax to the effective equilibrium with $\langle\sigma_z\rangle \to 0$ when $h_z \sim 0$. Computing the magnetization at equilibrium in the x direction gives $\langle\sigma_x\rangle \sim \Delta/\omega_c \to 0$ when $\omega_c \gg \Delta$ [113], which suggests by analogy to the thermal formula in Eq. (2), a temperature for T_{eff} much larger than Δ_r. In the pseudo-equilibrium picture, the two states become equally populated as $\lambda_+ \sim \lambda_-$. In the quantum problem, this traduces the entrance to a strongly entangled and incoherent regime (we note the absence of Rabi oscillations even at short-time scales). This regime is also related to the Kondo regime of the spin-boson model, which concerns α closer to unity [7]. It is perhaps relevant to mention that the close analogy between increasing temperature and increasing the coupling with the environment at zero temperature, in the context of Rabi dynamics, has been

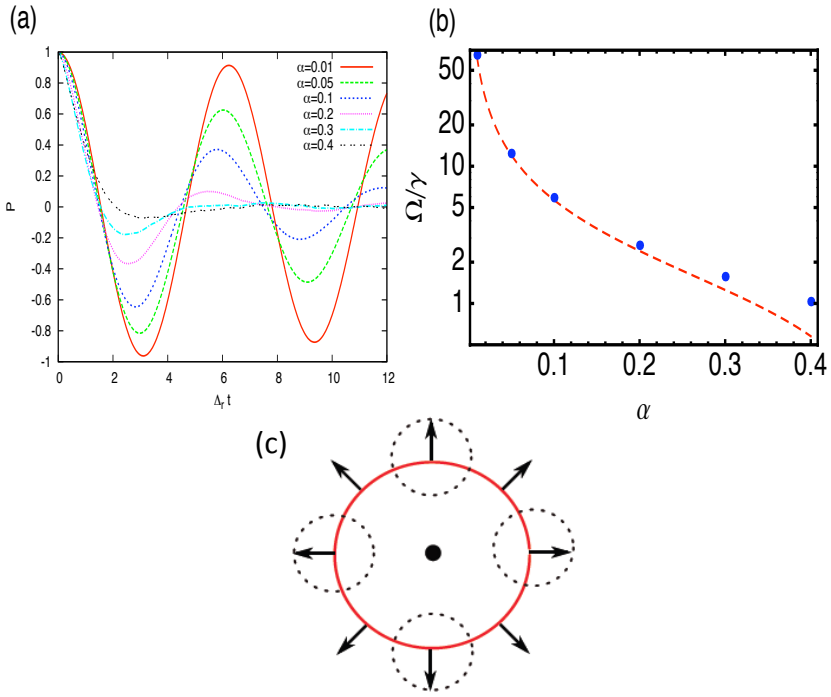

FIGURE 2 : Evolution of the Rabi dynamics $P(t) = \langle \sigma_z(t) \rangle$ as a function of the coupling with the environment with the first implementation of the stochastic Schrödinger equation approach with one stochastic field, in relation with Eq. (12). On the right, we plot the quality factor and compare with the form of Eq. (11) coming from the NIBA approximation. In Ref. [77], there is a precise comparison between the effects of increasing the coupling with the environment at $T = 0$ and of increasing the temperature. Recent developments with more than one stochastic fields allow to approach the point $\alpha = 1/2$ more closely [80]. However, the method still suffers for $\alpha > 1/2$ from convergence problems. For two spins, the quantum phase transition occurs for smaller coupling strengths allowing a very precise analysis of the dynamics in the localized phase [79]. (c) Cartoon of spin winding on the Bloch sphere in relation with Eq. (15) and Sec. 2.3

carefully analyzed with the stochastic Schrödinger equation approach [77] (see also Fig. 2). It should be noted that a similar (and universal) incoherent dynamics has been obtained in the synchronized regime of two spins using the stochastic Schrödinger approach [78].

2.3. Topology on the Bloch-Poincaré sphere and Dynamical Measurement for a half Floquet time period

Let us now address specifically the case of an arbitrary field on the Bloch sphere, following Refs. [80, 116] :

$$\hat{H} = -\frac{1}{2}\mathbf{d}\cdot\boldsymbol{\sigma}, \tag{15}$$

where $\mathbf{d} = (H\sin\theta\cos\phi, H\sin\theta\sin\phi, H\cos\theta)$. Recent experiments in quantum circuits have measured directly the Berry phase [117] or Chern number associated with a given spin path on the sphere [119, 120]. Let us perform a path from north to south pole on the sphere, meaning the polar angle changes from 0 to π and the azimuthal angle ϕ stays zero, and $\mathbf{d} = (\Delta, 0, h_z) = H(\sin\theta, 0, \cos\theta)$. One can adiabatically follow the ground state of the spin such that

$$|g\rangle = e^{-i\phi}\cos\frac{\theta}{2}|\uparrow\rangle_z + \sin\frac{\theta}{2}|\downarrow\rangle_z. \tag{16}$$

The Berry connection of the ground state $|g\rangle$ can be computed in a simple way and one finds $A_\phi = \langle g|i\partial_\phi|g\rangle = \cos^2(\theta/2)$ and $A_\theta = \langle g|i\partial_\theta|g\rangle = 0$. The Berry curvature then reads :

$$F_{\phi\theta} = (\partial_\phi A_\theta - \partial_\theta A_\phi) = (1/2)\sin\theta. \tag{17}$$

($F_{\phi\theta}$ would take the same form for another gauge choice of $|g\rangle$ in terms of the phase ϕ.) We obtain the Chern number :

$$C = \frac{1}{2\pi}\int_0^{2\pi} d\phi \int_0^{\pi} d\theta F_{\phi\theta} = 1. \tag{18}$$

A non-zero Chern number $C = 1$ reflects the fact that the total magnetic flux through the Bloch sphere is non-zero. This is due to a magnetic monopole that is trapped inside the Bloch sphere, which gives rise to the magnetic field $\mathbf{d}$. As shown in Fig. 2, this Chern number has also some interpretation of a winding number on the Bloch sphere due to the azimuthal symmetry of the problem [80]. The π-Berry phase of a spin-1/2 could also be recovered. We compute the phase that the ground state $|g\rangle$ acquires along a closed path around the equator ($\theta = \pi/2, \phi \in [0, 2\pi]$) such that $\gamma = \int_0^{2\pi} d\phi A_\phi(\phi, \theta = \pi/2) = \pi$. Using Stokes theorem, this can also be expressed in terms of the Berry curvature as $\gamma = \int_0^{2\pi} d\phi \int_0^{\pi/2} d\theta F_{\phi\theta} = \pi$. The important point is that for the particular protocol from north to south pole, one can relate the Chern number with a bi-partite measurement of observables on the sphere. More precisely, using the Hellmann-Feynman theorem, $C = -1/2[\cos\theta]_0^{\pi} = -1/2\,(\langle\sigma_z\rangle(\theta = \pi) - \langle\sigma_z\rangle(\theta = 0))$, as long as the magnetic field sweep is performed slowly enough to remain adiabatic [80]. A Chern number 1 can be interpreted in terms of a winding number on a sphere. This Chern number has been measured in recent experiments with superconducting circuits [119, 120]. Experiments in ultra-cold atoms have also measured the Chern number related to Bloch bands [121, 122, 123].

We can now focus on the robustness of the Chern number in the ohmic spin-boson model, applying the same protocol. Remarkably, we find that the quantization of the Chern number subsists until large couplings with the environment. More precisely, in the presence of the bath, the ground state can be generalized as [80] :

$$|g\rangle = \frac{1}{\sqrt{p^2+q^2}}\left(pe^{-i\phi}|\uparrow\rangle_z \otimes |\chi_\uparrow\rangle + q|\downarrow\rangle_z \otimes |\chi_\downarrow\rangle\right). \tag{19}$$

Here, $|\chi_\uparrow\rangle$ and $|\chi_\downarrow\rangle$ correspond to the two bath states associated with the two spin states. The first observation is that $\langle g|\sigma_z|g\rangle = (p^2 - q^2)/(p^2 + q^2)$. Now, we can use exact calculations [113] to check that close to the north pole and south pole, due to the fact that the transverse field $\Delta = H\sin\theta = 0$ vanishes, $\langle\sigma_z\rangle = \cos\theta$. The bath then has no effect at the north and south poles (meaning $p = \cos\theta/2$ and $q = \sin\theta/2$), and from the bi-partite definition of the Chern number, we predict that as long as one is in the delocalized phase of the spin-boson model ($\alpha < 1$) then the Chern number C remains quantized. In a recent paper [80], we have checked this point using a variational approach [195, 196]. Interestingly, we observe that the quantum phase transition in the ohmic spin-boson model at $\alpha = 1$ is characterized by a divergence of the Berry curvature at the equator, where the field h_z is small. More precisely, the Fermi liquid ground state of the ohmic spin-boson model is characterized by $\langle g|\sigma_z|g\rangle \sim h_z/\Delta_r = H\cos\theta/\Delta_r$ at small fields h_z [14], with $\Delta_r = \Delta(\Delta/\omega_c)^{\alpha/1-\alpha}$ and $\Delta = H\cos\theta$. Close to the equator where $\theta = \pi/2$ then we find [80] :

$$-\partial_\theta\langle g|\sigma_z|g\rangle \sim \left(\frac{\omega_c}{H}\right)^{\frac{\alpha}{1-\alpha}}. \tag{20}$$

Identifying $C = \int_0^{\pi} d\theta F_{\phi\theta} = -(1/2)\int_0^{\pi} d\theta(\partial\langle g|\sigma_z|g\rangle/\partial\theta)$, then the divergence of the spin susceptibility at the quantum phase transition [64] leads to a divergence of the Berry curvature at the equator, at the quantum phase transition $\alpha \sim 1$. We note that such a divergence of the spin susceptibility is expected to subsist for sub-ohmic environments [87, 89]. Other aspects of dissipative effects on the Berry phase of a spin-1/2 particle with a different time-dependent protocol) has been studied in Ref. [197].

Let us address a realistic protocol where one changes the polar angle linearly with time $\theta = vt$. The final time of the protocol is $t_{final} = \pi/v$. In relation to driven Floquet systems, periodic in time, note that this protocol focuses on half of a Floquet period. By increasing the velocity of the protocol v, one expects an adiabatic to non-adiabatic crossover when the final time t_{final} is equal to $1/\Delta_r$ (see Fig. 3 for example). More precisely, at the north pole the spin starts in the $|\uparrow\rangle_z$ state. The typical time to flip the spin from $|\uparrow\rangle_z$ to $|\downarrow\rangle_z$ based on Sec. 2.2 is of the order of $1/\Delta_r$; therefore, one expects a crossover in the bi-partite measurement $-1/2[\cos\theta]_0^{\pi} = -1/2\,(\langle\sigma_z\rangle(\theta = \pi) - \langle\sigma_z\rangle(\theta = 0))$ from 1 to 0 when $t_{final} \sim 1/\Delta_r$ or equivalently $v \sim \Delta_r$. This point has been explicitly recovered using the stochastic Schrödinger equation method [80]. It is important to note that formally

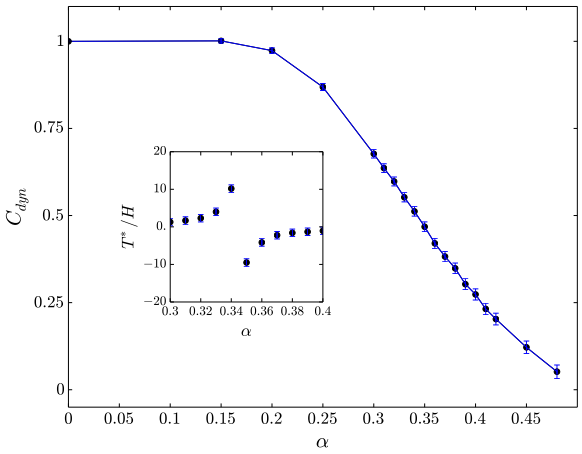

FIGURE 3 : Result obtained from the Stochastic Schrödinger Equation showing that the "non-adiabatic" Chern number C_{dyn} can become non-quantized and be strongly reduced (compared to the equilibrium quantized Chern number $C = 1$) when increasing the dissipation strength ; here $\nu/H = 0.08$ and $H/\omega_c = 0.01$ [80]. The crossover occurs when $\Delta_r \sim \nu$ since $C = C_{dyn} + O(\nu/\Delta_r)$. (inset) We show the effective temperature T_{eff} (defined as T^* for this particular protocol). There is an inversion of population when $C_{dyn} = 1/2$ and the environment produces an effective field compensating for the applied field. In Sec. 2.4, we describe a simple toy mean-field model to describe this quantum dynamo effect. It is important to note that this effect occurs for half a Floquet time period, and therefore on short time scales.

there is no disagreement with the fact that the equilibrium Chern number remains quantized to one. More precisely, defining the dynamical observable $-1/2[\cos\theta]_0^\pi = -1/2(\langle\sigma_z\rangle(\theta=\pi) - \langle\sigma_z\rangle(\theta=0))$ as a dynamical or non-equilibrium "Chern number" C_{dyn}, then we can show $C = C_{dyn} + O(\nu/\Delta_r)$ [116, 80].

Note that to reproduce quantitatively these results using a master equation in the weak-coupling sense is not so straightforward, since the $Q_2(t)$ function cannot be evaluated using the ground state of the environment. There is production of 'photons' in the environment, compensating for the applied magnetic field ; this effect will be described using a mean-field toy model in Sec. 2.4. Notice that for a given value of ν, when increasing α, one can observe a crossover between $C_{dyn} = C = 1$ to $C_{dyn} = 0$ when $\nu \sim \Delta_r$. The point corresponding to $C_{dyn} = 1/2$ implies that the environment screens the applied field such that $\langle\sigma_z\rangle(\theta=\pi) = 0$ and the effective temperature T_{eff} at the end of the protocol (referred to as T^* in Fig. 3 for this particular protocol) becomes infinity. Increasing α, then C_{dyn} becomes zero and there is an inversion of population, meaning that one observes negative (absolute) temperature. The entanglement entropy of the spin with the environment then shows a maximum when tracing out the environment and focusing on $S = -\mathrm{Tr}(\hat{\rho}\log\hat{\rho})$ [80].

At the Toulouse point $\alpha = 1/2$, using the Schwinger-Keldysh formalism on the effective resonant level model [80], we recover the same crossover when comparing the final time π/ν with the typical time scale $1/\Gamma = 1/\Delta_r$ where $\Gamma = H^2/\omega_c$ is the width of the resonant level. The occupation of the resonant level is related to the spin magnetization. In the limit of fast protocols, where $\nu \gg \Gamma$, then the dynamical Chern number becomes zero. The spin stays in the state $|\uparrow\rangle_z$ by analogy with the quantum phase transition at equilibrium at $\alpha \sim 1$. Note, however, that for an adiabatic protocol $\nu \ll \Gamma$, we expect the dynamical Chern number $C_{dyn} = 1 = C$. For $\omega_c \to +\infty$, treating the deviation from the Toulouse limit at a mean-field level, we note a scaling behavior $C_{dyn} \propto u$ and $u \propto (1/2 - \alpha)$ close to the Toulouse point, with a slope that becomes very steep for small $\nu/H \ll 1$, characterizing the emergence of a dynamical type Fermi liquid behavior [80].

We emphasize that this protocol has been realized in superconducting circuits [119, 120] and the presence of quite large dissipation can now be achieved using transmission lines and Josephson circuits [51, 36, 37, 42]. Karplus-Luttinger type equations have been used to measure the Chern number in ultra-cold atoms [121]. It would also be relevant perhaps to explore Caldeira-Leggett type dissipation on this protocol. It is also important to mention that a dynamical topological phase transition has been recently observed in ultra-cold atoms [198].

2.4. Solvable Mean-Field Stochastic Approach : Quantum Dynamo effect and Quantum Spin Relaxation

One can build an effective mean-field model to have another understanding of the preceding results. We refer to this effect as a quantum dynamo effect (rotating the spin on the Bloch sphere produces excitations, or artificial photons, in the environment).

More precisely, we can interpret the effect of the boson bath as an effective magnetic field $\langle\sum_k \lambda_k(b_k^\dagger + b_k)\rangle$ on the spin. Since the spin is driven at the frequency ν, then we can expect that the relevant bosonic modes will also be produced at this frequency. Therefore, we can build an effective one-mode model to describe more quantitatively this photon emission in the environment, following Ref. [80] :

$$\hat{H}_{eff} = \frac{H}{2}\cos(\nu t)\sigma_z + \frac{H}{2}\sin(\nu t)\sigma_x + \frac{\lambda}{2}\sigma_z(b+b^\dagger) + \nu b^\dagger b. \tag{21}$$

We obtain coupled equations of motion for the spin and the bosonic mode operator. The spin obeys classical Bloch equations similar to Eq. (13), and the bosonic environment satisfies

$$\frac{1}{\nu^2}\partial_t^2 h_{ind} + h_{ind} = -\frac{\lambda^2}{\nu}\sigma_z(t), \tag{22}$$

and $h_{ind} = \lambda\langle b + b^\dagger\rangle$. Let us consider the short-time limit where we assume to be in a non-adiabatic limit $\Delta = H\sin(\nu t) \sim H\nu t \ll \nu$ (the time is sufficiently short such that $H\nu t \ll \nu$). The spin will spend some time at the north pole where $\langle\sigma_z(t)\rangle = 1$. The physics for the environment becomes then very similar to shifted oscillators, where $h_{ind} \sim -\lambda^2/\nu$. In fact, one can check numerically this form of h_{ind} at the final time of the protocol [80]. We note that Eq. (22) becomes identical to that of a driven oscillator of frequency ν in an external field $-\lambda^2/\nu$. Here, the strength of the drive increases with the spin-bath coupling. Therefore, by increasing the spin-bath coupling, one expects $h_{ind} > H$. Now, we can fix the spectral function of the environment or λ such that $|h_{ind}|$ becomes larger than the applied field H for a critical value of α of the order of $1/2$, for example by fixing $\lambda = \sqrt{2\alpha\nu H}$ and $\lambda^2/\nu = 2\alpha H$. Then, we reproduce similar results as those obtained close to the Toulouse limit precedingly. At $\alpha = 1/2$, the total field $(H + h_{ind}) = 0$ and close to $\alpha = 1/2$, the effective field vanishes as $H(1-2\alpha)$, meaning $\langle\sigma_z(\theta = \pi)\rangle \propto u$.

Now, we would like to address the question of the spin relaxation to equilibrium in dissipative quantum spin chains. We note that various works have studied theoretically the phase diagram and dynamical properties of dissipative quantum Ising models [39, 80, 98, 102, 103, 104, 105, 130, 131]. Let us consider a solvable mean-field quantum Ising spin model. We focus on a system of M interacting spins, which are coherently coupled to one common bath of harmonic oscillators :

$$\hat{H} = \frac{\Delta}{2}\sum_{p=1}^{M}\sigma_p^x + \sum_{p=1}^{M}\sum_k \lambda_k e^{ikx_p}\left(b_{-k}^\dagger + b_k\right)\frac{\sigma_p^z}{2} - \frac{K}{M}\sum_{p\neq r}\sigma_p^z\sigma_r^z + \sum_k \omega_k b_k^\dagger b_k. \tag{23}$$

This model can be simulated in ultra-cold atoms [38, 39, 40], ion traps [132], with polar molecules [133] and in quantum electrodynamics circuits [134, 135]. Here, we discuss real-time dynamics close to the quantum phase transition using a solvable mean-field dynamics and with the stochastic Schrödinger equation approach which has already provided conclusive results for Kibble-Zurek physics [80]. Without dissipation, this model exhibits a mean-field like second-order transition at zero temperature when $K = \Delta/2$. The quantum phase transition separates a paramagnetic phase to a ferromagnetic phase with Ising long-range correlations in the z direction. Again, we assume an ohmic form for the spectral function and take $\omega_k = \nu|k|$, where ν represents the velocity of the sound modes. Using a unitary transformation [39], we find that the environment has two effects on the Hamiltonian, a renormalization of the transverse field into Δ_r similar to the one spin situation, and a renormalization of the spin-spin interaction. The renormalization of the spin exchange K_r due to the bosonic environment is analogous to the Ruderman-Kasuya-Kittel-Yosida interaction in Kondo lattices [14, 199] and can occur in light-matter systems [200].

To make a link with the quantum dynamo effect above and the Dicke model in quantum optics [127], assuming long-range coupling between spins, it is convenient to envision the model as a giant collective spin : $\tau_z = \sum_p \frac{\sigma_p^z}{2}$ and $\tau_x = \sum_p \frac{\sigma_p^x}{2}$. The quantum phase transition can be understood defining an effective Hamiltonian

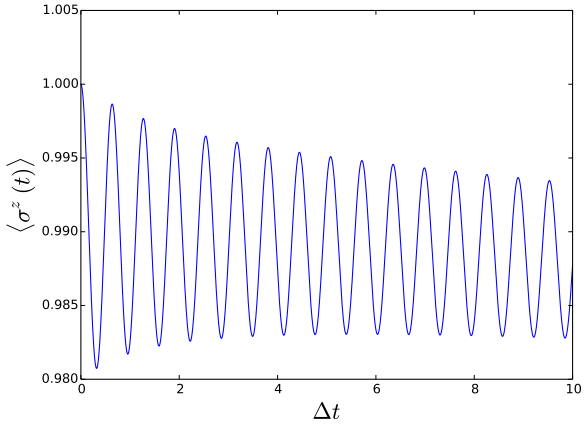

FIGURE 4 : Magnetization $\langle \sigma^z \rangle = \langle \sigma^z_p \rangle$ in the mean-field Ising spin chain far in the ferromagnetic phase using the NIBA approximation of Eq. (27). Parameters are fixed to $\Delta = 1$, $w_c = 3$ and $K_r = 10$. The transverse field produces small oscillations around the equilibrium value.

$\hat{H}_{eff} = \Delta_r \tau_x - \frac{K_r}{M}(\tau_z)^2$. We can then introduce the Holstein-Primakoff transformation : $\tau_x = b^\dagger b - M/2$ and $\tau_z = \sqrt{M}(b + b^\dagger)$, such that the Hamiltonian takes the simple form (up to a constant)

$$\hat{H}_{eff} = \Delta_r b^\dagger b - K_r(b + b^\dagger)^2 = (\Delta_r - 2K_r) b^\dagger b - K_r(b^2 + (b^\dagger)^2). \tag{24}$$

For $2K_r > \Delta_r$, $\langle b^\dagger b \rangle \neq 0$ and $\langle \tau_x \rangle$ will progressively diminish in the Ising ordered phase (the transverse magnetization $\langle \tau_x \rangle$ shows a crossover at the transition). Note that a coupling with a bosonic Gaussian bath can be included in such Dicke-type models allowing for a rigorous treatment of non-Markovian effects at low temperatures [128]. Dicke type models can also result in novel glassy phases [129] and exotic relations between fluctuations and entanglement at a quantum phase transition [201]. The dissipative quantum Ising model can be studied using an effective ϕ^4 theory and Monte Carlo numerical approaches [102, 103, 104, 105]. In the case of short-range spin correlations, the dissipation is expected to deeply affect the dynamical exponent z at the transition [102, 103, 104] ; in contrast, here the transition is mean-field like due to the long-range interactions [80]. Coupling the spin array to the environment following Ref. [39] and integrating out the Gaussian environment, then we can derive the closed equation starting from the paramagnetic phase (where the choice of mapping is appropriate) :

$$\frac{d^2\langle \tau_z(t) \rangle}{dt^2} \approx -\Delta^2_{eff} \langle \tau_z(t) \rangle - \int_0^t dt' \alpha(t - t') \frac{d}{dt'} \langle \tau_z(t') \rangle, \tag{25}$$

and $\alpha(t - t')$ is related to an effective kernel defining dissipation in relation with the spectral function [39]. In the paramagnetic phase, then we predict a renormalization of the Rabi frequency :

$$\Delta_{eff} \sim \Delta_r \left(1 - 2\frac{K_r}{\Delta_r}\right). \tag{26}$$

Treating the last term in a Markovian manner as $\sim -\eta d\langle \tau_z \rangle / dt$ would suggest an exponential relaxation of the Rabi oscillations in the paramagnetic phase. Approaching the transition, this analysis would suggest a purely exponential relaxation towards equilibrium with a relaxation time that would diverge for $\alpha = 0$ (in accordance with mean-field theories close to the critical temperature $T = T_c$). A similar analysis has been pushed forward in relation with ultra-fast dynamics in high-Tc superconductors [136]. By Fourier transform, dissipation effects in Eq. (25) scale linearly with frequency (in agreement with the Korringa-Shiba relation [8, 141], which will be studied in detail in Sec. 3).

To study the dynamics of $\langle \sigma^z(t) \rangle = \langle \sigma^z_p \rangle$ in the ferromagnetic phase and to make a connection with preceding sub-sections, we can also derive a closed equation of motion for the mean-field spin dynamics in the framework of

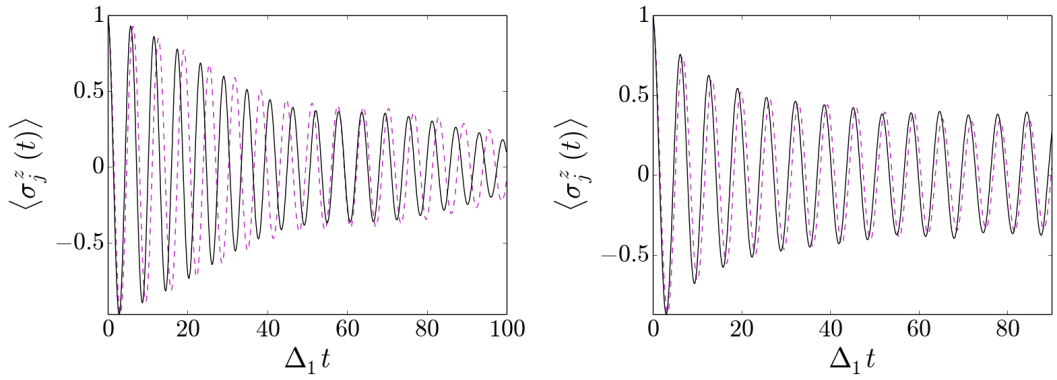

FIGURE 5 : (Dynamics of $\langle \sigma_1^z \rangle$ and $\langle \sigma_2^z \rangle$ for $\alpha = 0.01$ (Left), $\alpha = 0.05$ (Right) with $\Delta_2/\Delta_1 = 1.1$, $\omega_c = 20\Delta_1$, $K = 0$.

the well-known NIBA approximation [8, 9]. One gets

$$\partial_t \langle \sigma^z(t) \rangle = -\Delta^2 \int_{t_0}^{t} ds \langle \sigma^z(s) \rangle \cos\left[\frac{Q_1(t-s)}{\pi}\right] \exp\left[-\frac{Q_2(t-s)}{\pi}\right] \cos\left(K_r \int_s^t ds' \langle \sigma^z(s') \rangle\right). \tag{27}$$

Numerical results suggest that small oscillations around the equilibrium magnetization value can still take place in the ferromagnetic phase (see Fig. 4). Approaching the quantum phase transition from the ferromagnetic side, the spin relaxation time becomes larger than typical time scales accessible in the simulations.

2.5. Synchronization Revival from an environment

Now, we show an interesting effect of the environment in the context of spin dynamics and synchronization of two spins, obtained with the stochastic approach [80]. Synchronization mechanisms have been studied in the context of two spins [90, 137] and an ensemble of Josephson-coupled harmonic oscillators by analogy with circuit QED arrays [139]. Many-Body versions of synchronization have also been explored in superconducting systems [202]. It is important to mention that synchronization mechanisms have attracted a lot of attention recently, at the frontier between physics and neuroscience, and more precisely in the context of neural synchronization and the Kuramoto model, with some relation with Josephson junction arrays and the Brownian motion, as well as spin networks [139, 140].

A synchronization regime was recently observed in Ref. [138] in the oscillatory dynamics of a mixture of bosonic and fermionic species. The authors suggested that the appearance of this synchronization regime was due to the coupling of the relative motion of the two clouds to a dissipative environment. We build a toy model related to this problem by restricting the dynamics of each species to only two motional states (essentially, the left top and right top of an harmonic trap). The resulting Hamiltonian is analogous to two coupled spins-1/2 impurities and reads :

$$H = \frac{\Delta_1}{2}\sigma_1^x + \frac{\Delta_2}{2}\sigma_2^x - K\sigma_1^z\sigma_2^z + \sum_k \left[\left(\sigma_1^z - \sigma_2^z\right) \frac{\lambda_k}{2} (b_k + b_k^\dagger) + \omega_k b_k^\dagger b_k \right], \tag{28}$$

where the operator σ_p^z describes the position of the cloud $p \in \{1, 2\}$ (either left or right), while the tunneling term σ_p^x switches the position from left to right or from right to left. $\Delta_1 \neq \Delta_2$ are the two bare frequencies of the two species. K denotes the interaction strength between the two spins. We assume that the relative motion of the two species is coupled to an ohmic bath.

Fig. 5 shows the dynamics of the two spins, with initial state $|\uparrow_z, \uparrow_z\rangle$ for increasing strengths of the system-environment coupling (from left to right and top to bottom). At very weak coupling ($\alpha < 0.02$), we observe an asynchronous decay of the two spin oscillations towards an equilibrium state with $\langle \sigma_1^z \rangle = \langle \sigma_2^z \rangle = 0$. Interestingly,

we remark that the damping of the oscillations is temporarily smaller when the oscillators are in phase, signaling the onset of synchronization. In this regime of very weak coupling, the life-time of the oscillations diminishes with increasing α. Then, above a certain (small) coupling strength of the order of 0.05, we observe the appearance of long-lived synchronized oscillations of the two spins. In this regime, the two spins oscillate at the same frequency and these oscillations acquire a seemingly infinite life-time. Other initial conditions do not lead to the same synchronized regime, signaling the presence of an attractor in the phase space. To show that these results are not induced by the direct interaction between spins, we fix $K = 0$ in Fig. 5. Other results have been presented in Ref. [80] and the limit of large K_r has been discussed in Ref. [90].

3. Quantum Simulators

In this Section, we present specific simulators of quantum impurity systems with Ohmic dissipation, in mesoscopic systems, cQED hybrid devices, and ultra-cold atoms. We address other fundamental aspects such as the importance of Korringa-Shiba relation (regarding the two-time anti-symmetric correlation function $\langle\sigma_z(t)\sigma_z(0)\rangle$ which now relates to the dynamical spin susceptibility and decays as $1/t^2$ at long times, whereas $\langle\sigma_z(t)\rangle$ of Sec. 2 relates to the symmetrized part [77]) and analogies to Kondo and Quantum Brownian Motion in and out of equilibrium. In relation with Josephson circuits and Kondo physics of light, we present an AC analogue of the Friedel's phase. We also discuss some engineering of a quantum microscope (spin-1/2 impurity) in ladder systems to probe the Mott-superfluid transition. Then, we make connections with driven Floquet systems allowing to engineer artificial gauge fields and measure chiral currents [172, 173, 174].

3.1. Josephson Circuit and Kondo Physics of Light : analogue of Friedel physics in the AC limit

The dissipative spin-boson model can be realized in noisy charge qubits built of mesoscopic quantum dots or Cooper pair superconducting boxes [203]. A charge qubit can be seen as a spin-1/2 object corresponding to the two degenerate charge states forming the low-energy sub-space [204, 205]. Gate voltages can control the two charge states and allow to realize an effective magnetic field h_z and Δ corresponds to the tunneling amplitude between the (superconducting) box and the lead(s) or the Josephson coupling energy of the junction.

If the gate source is placed in series with an external resistor, which can be modeled by a long LC transmission line, this may describe the spin-boson model with ohmic dissipation. A long transmission line also refers to a one-dimensional Josephson array [36, 37], one-dimensional Luttinger liquid or a metallic carbon nanotube [43, 50], a 1D BEC [38, 41]. The spin-boson model can also be derived when coupling a quantum dot to a boson and fermion bath [33, 64, 206]. Charge measurements provide generally the quantity $\langle\sigma_z\rangle$, which represents the occupation of the dot or island. In a ring geometry, the application of a magnetic flux generates a persistent current which is proportional to $\langle\sigma_x\rangle$ [32]. Recent realizations [51, 207] of the model involve flux qubits ; transmon or Xmon qubits, could also offer a long lifetime [208, 209]. These nano-systems also allow to address non-equilibrium transport at a given quantum phase transition, both theoretically and experimentally [43, 50, 210, 211].

Below, we describe a Josephson setup realizing the spin-boson model with tunable Ohmic dissipation in the microwave regime [144, 145, 212]. The two-level system corresponds to the two-charge states on a mesoscopic superconducting system (an extra pair on the left or on the right box, see Fig. 5 for an illustration). This system can realize an analogue of the Kondo effect for photons and we propose an AC analogue of the relation between DC conductance and Friedel's phase for electrons in Kondo systems [213], in the context of microwave light. Note that an AC potential, or input microwave signal, is an example of Floquet perturbation periodic in time.

Quantum excitations in the two long transmission lines are described by collection of harmonic oscillators (zero-point fluctuations) ; b_{lk} and b_{rk} destroy an 'excitation' in mode k in the left and right transmission lines, respectively. This produces zero-point fluctuations reminiscent of vacuum in free space ; the main difference is that in one-dimensional waveguides, the quantization of energy requires only 'one-polarization' of bosons. To study transport of microwave photons, we introduce the symmetric b_{sk} and antisymmetric b_{ak} combinations of b_{lk} and b_{rk}, in relation with Fig. 6. Similar to a quantum dot coupled to electron leads in the Kondo regime [213], one can engineer that only one combination (here, the antisymmetric one), couples to the effective spin describing the two charge states on the mesoscopic island. After a unitary transformation, the Hamiltonian takes the form [144] :

$$\hat{H} = \sum_{k>0} v_a|k|\left(b^\dagger_{ak}b_{ak} + \frac{1}{2}\right) - \frac{h_z}{2}\sigma_z - \frac{E_J}{2}\sigma_x - \sum_{k>0}\lambda_k(b_{ak} + b^\dagger_{ak})\frac{\sigma_z}{2}. \tag{29}$$

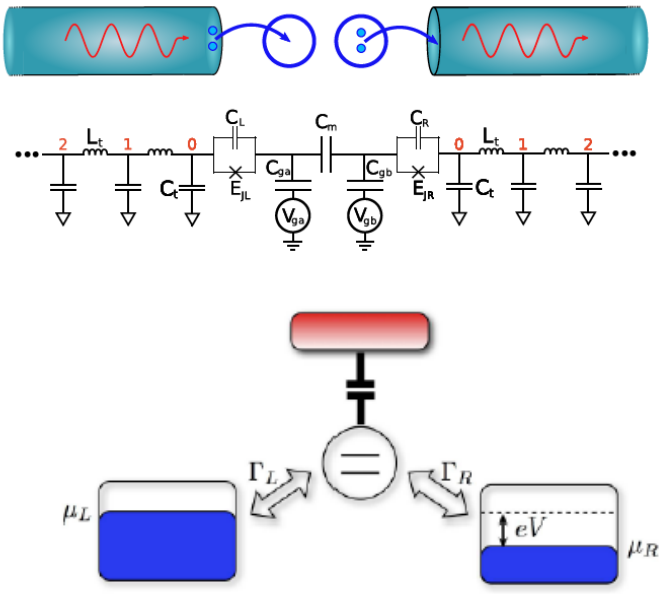

FIGURE 6 : (Top) Josephson junction circuit in the microwave regime as a quantum simulator of Kondo Physics of Light [144, 145]. The original setup was based on a double-dot superconducting charge qubit, in the presence of a finite capacitance C_m between boxes (islands) [204, 205]. The circuit allows to realize a perfect Rayleigh transmission at resonance with a large photonic bandwidth related to the Kondo energy scale [144]. We also try to relate the perfect transmission of the signal with a Friedel phase in the AC regime. In addition, the circuit allows to explore the strong-coupling limit, inelastic effects and the vicinity of the quantum phase transition in the spin-boson model [145]. We note recent efforts to build such a circuit using flux qubits [51, 207]. Transmon [208] or Xmon [209] qubits and other Josephson circuits [36, 37] could also offer a long lifetime. (Bottom) Quantum Hybrid Simulator coupling a cavity or cQED environment in red with a mesoscopic quantum dot circuit in blue, as studied experimentally in Ref. [152], in relation with some theoretical efforts [148, 149, 150]. The system exhibits a capacitive coupling between the cavity and the charge on the quantum dot. We also mention current efforts in graphene quantum dots [153].

We focus on the propagation of a field from left to right and focus on the right-moving modes with $k > 0$. The spectral function of the environment is ohmic $J(\omega) = \pi \sum_{k>0} \lambda_k^2 \delta(\omega - \omega_k) = 2\pi\alpha\omega e^{-\omega/\omega_c}$ where $\omega_c \gg E_J$ represents the high-frequency plasma frequency cutoff and the dissipative parameter α is given by

$$\alpha = \frac{2R}{R_Q}(\gamma_l^2 + \gamma_r^2). \tag{30}$$

Here, $R_Q = h/(2e)^2 = 2\pi/(2e)^2$ denotes the quantum of resistance where $2e$ is a charge of a Cooper pair, R is the resistance of each transmission line and γ_l and γ_r represent effective dimensionless couplings of the qubit with the left and right transmission lines (γ_l^2 and γ_r^2 are of the order unity after a unitary transformation [144]).

In the coherent regime, essentially for a range of α parameters ($0 \ll \alpha \ll 0.5$) similar to the underdamped Rabi oscillations, the spin is described by the following dynamical spin susceptibility which describes the response to an input AC field

$$\chi(\omega) = \frac{\omega_K}{\omega_K^2 - \omega^2 - i\gamma(\omega)}, \tag{31}$$

where $\omega_K = T_K = \Delta_r$. This equation has been derived in the supplementary material of Ref. [144]. This form has been checked with numerical renormalization group arguments [214]. Using a combination of input-output theory [154] and Bethe-Ansatz approach [113] to describe the transport of input and output photon fields, we predict that the broadening takes the form [144] $\gamma(\omega) = \omega_K J(\omega)$ until frequencies of the order of ω_K, in agreement with the Korringa-Shiba relation in the low-frequency domain [141]

$$\mathrm{Im}\,\chi(\omega)|_{\omega\to 0} = 2\pi\alpha\omega(\mathrm{Re}\,\chi)^2(\omega = 0). \tag{32}$$

In particular, one can reach analytically an equation similar to the underdamped regime of Sec. 2 :

$$\langle\sigma_z(\omega)\rangle(-\omega^2+\omega_K^2-i\gamma(\omega))=\omega_R\gamma_l\langle V_l^{in}\rangle. \tag{33}$$

The input field V_l^{in} in the left transmission line is defined as a coherent superposition ($b_{lk}+b_{lk}^\dagger$), and $\langle V_l^{in}(\omega)\rangle = V_{ac}\cos(\omega t)$ [144].

The novel aspect resides in the fact that in such geometries, the spin susceptibility can be measured through the transport of one photon in the circuit, leading to a many-body resonance in the elastic transmission [144]

$$t(\omega,P_{in})=-\frac{2i\gamma_r\gamma_l}{\gamma_l^2+\gamma_r^2}J(\omega)\chi(\omega,P_{in}). \tag{34}$$

Here, P_{in} is the averaged input power related to $\langle V_l^{in}\rangle$. For the spin-boson model with an emergent Fermi liquid behavior at low energies, we note $J(\omega_K)\chi(\omega_K)=i$ for $P_{in}\to 0$. Close to resonance, when $\omega=\omega_K$, an analogy with the unitary DC conductance in the Kondo regime of mesoscopic systems can be formulated as follows. Let us first remind the form of the DC conductance through a quantum dot in the Kondo regime [213]

$$G_{DC}=2\frac{e^2}{h}\sin^2(2\theta)\sin^2\delta, \tag{35}$$

where $\delta=\pi/2$ is the Friedel's phase acquired for a plane wave (here, at the Fermi energy or $\omega=0$) backscattered by the magnetic impurity, and θ measures the anisotropy between left and right probes (tunnel couplings). It is perhaps important to remind that from the T-matrix approach, one relates $-\pi T(\omega=0)=(1/2i)(e^{2i\delta}-1)$ [213]. The maximum of DC conductance then corresponds to a phase $2\delta(\omega=0)=\pi$ between an incident and a scattered wave packet. The phase $2\delta=\pi$ is reminiscent of the Friedel's phase such that due to the screening of the impurity and the Pauli principle in the case of electron reservoirs, then the wave function should have a node at the impurity site $x=0$, implying the rule between left and right going waves [215] $\psi(0)=\psi_L(0)+\Psi_R(0)=0$. This equality ensures that $\Psi_L(0)=e^{2i\delta}\Psi_R(0)=-\Psi_R(0)$. The spin channel is taken into account in the factor 2 in the DC conductance.

In the Josephson geometry, we also check the form $\sin(2\theta)=2\gamma_l\gamma_r/(\gamma_l^2+\gamma_r^2)$. For the microwave light, the transmission t is a transmission amplitude, referring to the ratio between the output and input signals (AC fields), and for frequencies close to ω_K [144] :

$$t(\omega\sim\omega_K,P_{in}\to 0)=|t|=\sin(2\theta). \tag{36}$$

The phase of the transmitted light signal is zero. For symmetric conditions, the transmission reaches unitarity. Now, if instead we focus on the reflection coefficient (ratio of the output and input fields in the left transmission line) [144] :

$$r(\omega,P_{in})=|r|e^{i2\delta}=1+2i\frac{\gamma_l^2}{\gamma_l^2+\gamma_r^2}J(\omega)\chi(\omega,P_{in}), \tag{37}$$

and at resonance, we find :

$$|r|e^{i2\delta(\omega=\omega_K)}=-\cos(2\theta)=\frac{\gamma_r^2-\gamma_l^2}{\gamma_l^2+\gamma_r^2}. \tag{38}$$

For $\gamma_l=0$, we recover the phase of an open line $\delta=0$ (and formally, $2\theta=\pi$) whereas for $\gamma_r<\gamma_l$, we find a phase of $2\times\pi/2=2\delta(\omega=\omega_K)$ and $\theta=0$. We notice that the same phase $2\delta=\pi$ occurs at resonance for the photon reflection, emphasizing the duality between zero-point fluctuations and electron-hole pairs in one dimension through bosonization [34, 35]. Writing the input and output signals in the left transmission line in terms of b_{lk} and $b_{lk}^\dagger$, then this phase can also be seen as the phase taken by a bosonic excitation in the left transmission line with wave-vector defined as $vk=\omega_K$. To summarize this part, the observation of a Kondo-type resonance in these microwave circuits can be established as follows. First, observe a many-body light shift :

$$\omega_K=E_J\,(E_J/\omega_c)^{\frac{\alpha}{1-\alpha}}\ll E_J. \tag{39}$$

Experimentally, this form of many-body frequency shift requires formally that the spectral function of the environment has an ultra-violet cutoff $\omega_c \gg E_J$ and an infra-red cutoff smaller than ω_R (see Eq. (21) of supplementary material of Ref. [144]). In the absence of Kondo physics (meaning $\alpha = 0$), the light resonance condition is fixed by the gap $\sim E_J$ separating the two states $\sigma_x = +1$ and $\sigma_x = -1$ of the spin (qubit). Second, the Friedel' s phase of $2\delta = \pi$ in the reflected light signal at the resonance frequency $\omega = \omega_K$ would also be a strong indication of Kondo physics.

We also note that the broadening of the elastic Rayleigh peak is much larger than in the weak dissipation limit [216, 207]. By increasing the input power power P_{in}, the evolution of the Mollow triplet [216] observed for weak dissipation remains an open question for larger dissipation regimes. Nevertheless, one can check that the scattering matrix around $\omega = \omega_K$ becomes non-unitary since $J(\omega_K)\,\mathrm{Im}\,\chi(\omega_K, P_{in}) < 1$, which hides the presence of additional inelastic corrections [144]. These inelastic Fermi-liquid corrections have also been studied by Goldstein *et al.* in a larger regime of α parameters (ultra-strong coupling limit close to the Kosterlitz-Thouless transition) [145] and also in a Rabi-Kondo laser-driven system [217]. We also note some theoretical efforts to describe quantitatively the scattering of bosonic waves in a many-body sense in solvable models [218, 219, 220, 221]. Furthermore, the exact non-Markovian dynamics of transmon qubits in open multi-mode resonators can be obtained from reduced Heisenberg-Langevin equations of motion, in which the effects of the (possibly lossy) electromagnetic environment are present via a classical Green's function [222]. Extensions of this model could include realizations of two-channel Kondo physics [156] with light, as recently observed for electrons [163, 164], or a single effective spin-1/2 in a cQED array [19, 22].

As described below in Sec. 3.3, hybrid systems comprising reservoirs of electrons as well as a cavity also offer a novel platform where light can probe the Kondo effect entangling a spin and conduction electrons. We summarize a few theory steps [148, 149, 150] in relation with current experiments [152, 153]. In Sec. 3.4, we also propose an analogue circuit in ladder systems where the spin-1/2 acts as a quantum microscope which can probe Mott-Superfluid transition in the environment.

3.2. Driven Quantum RC circuits, Topological Josephson Kondo Circuits and Berry Phase, Quantum Brownian Motion

Now, we investigate the AC regime more carefully in the limit of low-frequency (long-time limit).

A typical experimental system is a quantum RC circuit, shown in Fig. 7, consisting of a mesoscopic metallic island (cavity) tunnel-coupled to a metal (essentially, a two-dimensional electron gas or a one-dimensional Luttinger liquid, edge channel of the quantum Hall effect). The study of AC coherent transport was pioneered in a scattering approach by Büttiker, Prêtre and Thomas in 1993, where a charge relaxation resistance of $R_q = h/2e^2$ was predicted for a single-mode resistor [146]. In this experiment, the averaged charge $\langle Q\rangle = e\langle N\rangle$ on the island is measured in response to a small AC gate potential :

$$\frac{\langle Q(\omega)\rangle}{V_g(\omega)} = C_0(1 + i\omega C_0 R_q) + O(\omega^2). \tag{40}$$

Formally, we focus on time scales much longer than the typical RC time and we assume that the voltage is of the form $V_g(\omega) = V_{dc} + V_{ac}\cos(\omega t)$ with $(V_{ac}, \omega) \to 0$. The quantum RC circuit is drawn in Fig. 6 and has been successfully implemented in a two-dimensional electron gas and a quantized resistance of $R_q = h/2e^2$ was measured in *GaAs* [151]. This quantized resistance must be thought as a contact resistance between the mesoscopic island and the reservoir lead. Note that the factor 2 does not come from spin effects. This resistance must be thought as a quantum coherent effect analogous to a Fabry-Perot resonator, and occurs in fact for any transmission amplitude t (or reflection $|r|$) at the junction.

Coulomb blockade effects were first ignored and later they have been partially taken into account in a Hartree-Fock theory [223]. Using bosonization approach, we can include interactions in a non-perturbative manner. We also show a crossover at finite frequency ω, where the charge relaxation resistance changes from $h/2e^2$ to h/e^2 regardless of the mode transmission. All the technical details can be found in Ref. [147]. Here, we give a simple understanding to this crossover and we then make an analogy with the Kondo effect. Let us model the system by a one-dimensional line (see Fig. 5), the lead is between $-\infty$ and $-L$ and the quantum dot between $-L$ and 0. The level spacing on the quantum dot (cavity) is $\Delta = \pi v_F/L$, where v_F is the Fermi velocity. The Coulomb blockade

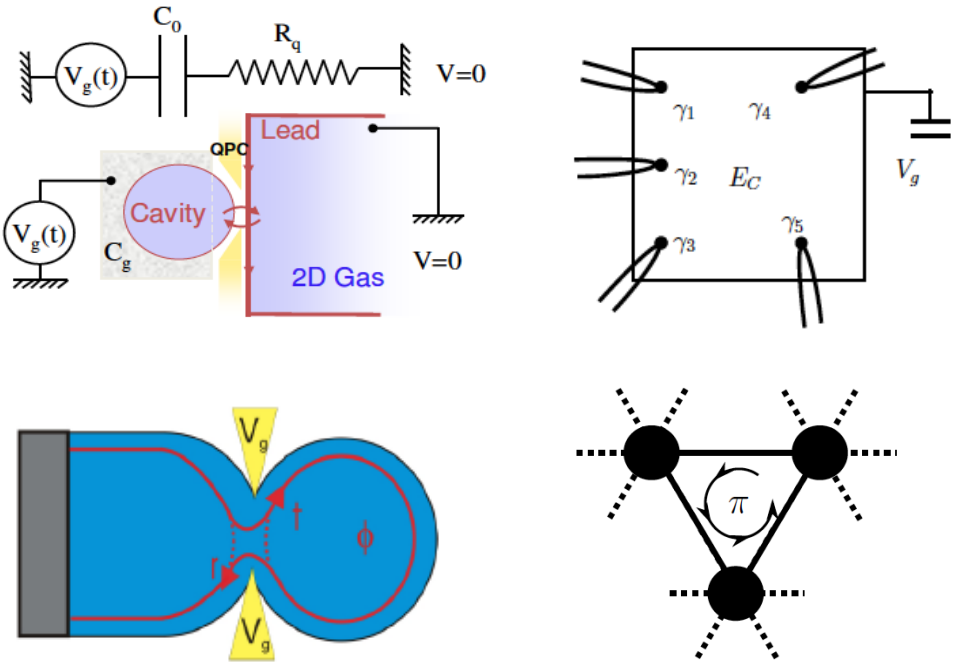

FIGURE 7 : Examples of Mesoscopic Circuits. (Top left) Quantum RC circuit [146] (from Ref. [147]) coupling a quantum dot (box or island, cavity) with an electron reservoir driven by an AC gate voltage as realized in *GaAs* [151]. For a metallic quantum dot, charge Kondo physics was recently realized with quantum Hall edge states [43], in an analogue circuit as Bottom Left, following theory [165, 166]. Universal quantized resistances can emerge for all transparencies as Fabry-Perot effects, maintaining the phase coherence ϕ. These large boxes also lead to a novel relation between charge relaxation resistance and Korringa-Shiba relation at low frequency [147]. (Top Right) Topological Mesoscopic Box with Majorana Fermions allowing to realize exotic multi-channel Kondo physics [156], at the charge degeneracy points [157, 158] and away from charge degeneracy [159, 160, 161]. This multi-channel Kondo physics also allows to make a connection with the quantum Brownian motion [155] and dual lattices with artificial gauge fields, which may reveal π phases due to pseudo-spin effects [157] (Bottom Right). The effect of artificial gauge fields leads to complex phenomena such as topological phenomena and Meissner physics [173, 182, 239], see Sec. 3.4, and is also in relation with Kuramoto models of coupled Josephson-junction systems studied in Neuroscience [139]. A quantum Brownian motion analogy was also addressed in the case of dissipative tunnel junction problems and Ramsey interferometry [52].

phenomena are treated exactly in an action and bosonization formalism [35] after integrating out all irrelevant modes. At perfect transmission, the system is then described by the action [147] :

$$S_0 = \frac{1}{\pi}\sum_n \phi_0(\omega_n)\phi_0(-\omega_n)\left[\frac{|\omega_n|}{1-e^{-2|w_n|L/v_F}} + \frac{E_c}{\pi}\right], \tag{41}$$

where $\omega_n = 2\pi T n$ denotes bosonic Matsubara frequencies ; the Boltzmann constant k_B is set to unity and $E_c = e^2/2C_g$ corresponds to the (bare) charging energy (Fig. 6). Here, the bosonic field ϕ_0 means $\phi(-L)-\phi(0)$, which is related to the charge on the dot through $C_0 V_g/e + \phi_0/\pi$. From this bosonic action, one can read the Green's function of the charge field ϕ_0, and immediately infer the response

$$\frac{Q(\omega)}{V_g(\omega)} = \frac{C_g}{1-\frac{i\omega\pi/E_c}{1-e^{2i\omega\pi/\Delta}}}. \tag{42}$$

The response vanishes each time the frequency ω hits a multiple of Δ, *i.e.* an eigenstate of the isolated island. At low frequency, we extract $C_0 = C_\mu$, where C_μ is the electrochemical capacitance corresponding to the classical

capacitance C_g in series with the quantum correction e^2/Δ, such that the Coulomb blockade vanishes for perfect transparencies at the junction. In the low-frequency limit, for $\omega \ll \Delta$, we also recover the universal resistance $R_q = h/2e^2$ (in units of $\hbar = 1$ then $h = 2\pi$). By increasing the size of the quantum dot, the response shows an oscillatory behavior for $\omega > \Delta$. We thus average over a finite bandwidth $\delta\omega$, such that $\omega \gg \delta\omega \gg \Delta$, and

$$\frac{Q(\omega)}{V_g(\omega)} = \frac{C_g}{1 - i\omega\pi/E_c}. \tag{43}$$

This leads to $R_q = h/e^2$, equal to the quantum of resistance R_K in Fig. 1 (this result can also be obtained directly from the action in imaginary time when $L \to \infty$).

This result can also be recovered using an analogy with the Kondo effect, following Matveev [165, 166], where two successive charge states on the metallic island can be identified to a macroscopic pseudo-spin. The two effective spin polarizations of conduction electrons must be associated to the 'metallic island' and 'lead' locations respectively. Using standard linear response theory, then one identifies $Q(\omega) = e^2 K(\omega) V_g(\omega)$ where [147]

$$K(t - t') = i\theta(t - t')\langle[N(t), N(t')]\rangle. \tag{44}$$

The spin analogy allows to relate K with the spin susceptibility χ of the underlying Kondo and Fermi liquid theory [6, 142]. The isotropic Kondo model is equivalent to the spin-boson model in the limit $\alpha \to 1$. Taking $\alpha = 1$ in the Korringa-Shiba relation of Eq. (31), one immediately recovers $R_q = h/e^2$. It is also interesting to observe the relation with Eq. (30), in the low-frequency domain. Such a charge relaxation resistance in large metallic dots with $\Delta \to 0$ has not yet been observed. We note that recent experimental progress has allowed to observe such a charge Kondo effect in DC transport [43]. This experiment involves (integer) quantum Hall edge states. If we generalize the calculation for an Abelian quantum Hall edge state with a filling factor ν (see Fig. 7), this gives the two (generalized) resistances $R_q = h\nu/(2e^2)$ and $R_q = h\nu/e^2$ [147]. The effect of a small zeeman field has been studied in Ref. [224].

Other and related important results have been established by Hamamoto *et al.* [225]. The quantum RC circuit has also close analogies with dissipative mesoscopic rings [226]. A generalization to the Anderson model has also been done in Refs. [227, 228] as well as for several conducting channels [229]. Moreover, considering a quite general cavity geometry with a single-channel lead, Ref. [230] has shown that the universal resistance $R_q = h/e^2$ is in fact more general than the specific form of the action (40) or the Anderson or Kondo underlying models, but applies generally as soon as the system is described at low energy by a Fermi liquid fixed point. In this case, the Korringa-Shiba formula can be derived on general grounds leading to the resistances $R_q = h/e^2$ and $R_q = h/2e^2$ depending only on whether the cavity has a dense spectrum or not. For a two-channel Kondo model subject to non-Fermi liquid corrections, using a Majorana description for the spin [231], one finds an increase of the charge relaxation resistance induced by the non-Fermi liquid behavior at larger frequencies [232]. The charge relaxation resistance has also been computed in mesoscopic topological superconducting circuits [233] and at the edges of two-dimensional topological insulators [234]. We also note recent efforts to consider real-time dynamics and charge relaxation in these interacting systems [235].

One-dimensional leads also allow, through a dissipative action proportional to $|\omega|$, a connection to the quantum Brownian motion addressed by Yi and Kane [155]. Let us consider a specific recent example of Fig. 7 with M one-dimensional leads described by a Luttinger theory (with Luttinger parameter K [34, 35])) tunnel coupled through a mesoscopic box, which comprises several topological superconducting wires possessing Majorana fermions at their extremities [236, 237]. The Hamiltonian takes the form [157, 158] :

$$\hat{H} = \hat{H}_{leads} + \hat{H}_{box} + \sum_{j=1}^{M} t_j e^{-i\chi} \psi_j^\dagger(0)\gamma_j + h.c. \tag{45}$$

Here, t_j is the tunneling amplitude between each lead and the box, $\psi_j(0)$ describes the electron operator in a lead j in the entrance of the mesoscopic box, γ_j represents a Majorana fermion in the mesoscopic box and in this expression χ is the superconducting phase conjugate to the number of Cooper pairs. The charging energy is hidden in H_{box} following Refs. [157, 158]. Away from charge resonance in the mesoscopic system, single-particle

transport is blockaded and one can apply a standard Schrieffer-Wolff transformation to re-write the tunneling terms in the bosonized language as [157]

$$\hat{H}_{SW} = -\sum_{j\neq k} \lambda_{j,k} \cos(\theta_j - \theta_k). \tag{46}$$

The phases θ_j describe the superfluid-type phases in the entrance of the box in each metallic lead (wire) [35] and one exactly takes into account the parity operator $p_j = i\gamma_j U_j$ where U_j represents a Klein factor in a wire j, which commutes with the total Hamiltonian [34, 238].

This problem also refers to the topological Kondo model first introduced in Refs. [159, 160] : one can identify an effective pseudo-spin as a product of two Majorana fermions [231] and therefore in the fermion picture H_{SW} makes link with a multi-channel Kondo model of the form $\sum_{j,k} \tilde{\lambda}_{j,k} \psi_k^\dagger(0)\psi_j(0)\gamma_j\gamma_k$. The word topological here can be understood from the fact that the spin is built from Majorana like excitations and from the fact that a channel anisotropy is irrelevant. By (also) considering attractive interactions in the leads (implying a Luttinger parameter $K > 1$), the system flows to a strong-coupling Kondo fixed point. An analogy with the quantum Brownian motion can be understood at the strong coupling fixed point of the Kondo model. The mode $\theta = (1/\sqrt{M})\sum_{j=1}^{M} \theta_j$ decouples from the Hamiltonian [157], and has a free evolution reflecting the charge quantization. One can then build an effective model for the remaining phase variables θ_j of a massless particle subject to dissipation (here, stemming from the electron-hole pairs in each lead) in a $(M-1)$ dimensional space. The minima of the potential form a (hyper)triangular lattice, and must satisfy that $\theta_j - \theta_k = 2n\pi$ where $n \in \mathbb{N}$. The (fractional) DC conductance at this strong-coupling fixed point is also in agreement with an in-coming wave equally flowing in all the leads.

At the charge degeneracy point, one can formulate a similar analogy to the Kondo model. More explicitly, according to the recent Ref. [157], we introduce a pseudo spin acting on the charge space in the box as $\tau^-|N+1\rangle = |N\rangle$. The model is mapped onto a M channel Kondo model [156]. In the strong-coupling fixed point limit (that can be reached for free electrons), as a reminiscence of the topological Kondo effect [159, 160, 161], one can build a connection to the same quantum Brownian motion. However, there is a difference : each minimum of the dual lattice is characterized by a (pseudo-)spin wave function : $(e^{-i\pi/M}|\uparrow\rangle_z + e^{i\pi/M}|\downarrow\rangle_z)$. Performing a loop with different neighboring directions in the dual lattice produces then an overall Berry phase $e^{i\pi} = -1$ (a site has M neighbors) [157]. This phase is drawn in Fig. 7. The presence of a pseudo-spin creates artificial gauge fields in the dual lattice. It is relevant to note that recent experiments in quantum cQED transmon circuits [182] and ultra-cold atoms [239] have engineered similar gauge fields. These gauge fields also emerge as artificial phase factors (such as Jordan-Wigner strings) in quantum field theories [240, 241]. At this strong-coupling fixed point, the DC conductance again is in agreement with an in-coming wave equally flowing in all the leads. We also identify a possible intermediate Kondo fixed point, for a Luttinger parameter $K = 1/2$, described by an intermediate phase shift $\delta = \pi/(M+2)$ in Eq. (34) obtained from the M channel Kondo model [157, 158].

This research is directly motivated by current efforts to realize and manipulate Majorana fermions in superconducting systems [242]. We also note the very recent related theoretical developments [243, 244]. It is also important to note that H_{SW} is connected to tunnel junction dissipative Kane-Fisher models and dynamical Coulomb blockade physics [44, 45]. In this respect, we would like to mention a relation between Ramsey interferometry at a tunnel junction, produced after two voltage pulses in time, and the current noise at zero frequency [52]. The relation has been first built for free electrons (coupled to a dissipative environment) and can be generalized for quantum Hall edge states and Luttinger systems. As an application studied in Ref. [52], we would like to mention that such a Ramsey protocol in time allows to probe the charging energy at the junction, already in the small resistance limit for the dissipative Ohmic environment. One can also draw a similar analogy with a dissipative quantum Brownian motion (but also including the feedback of voltage pulses in transport). We notice that dissipative effects can also reveal extra phase shifts at small resistances, and we may anticipate that similar effects will occur for quantum Hall edge states, similarly as for the charge relaxation resistance. In addition, two-time correlators in Luttinger liquids provide a connection between Loschmidt echo, Ramsey interferometry and quench-induced decoherence [56, 57].

3.3. Hybrid Systems, Quantum Browian Motion from non-linear Transport and Kondo Physics

Let us now extend the discussion to hybrid mesoscopic systems, and study the interplay between quantum electron transport and a circuit-QED environment [245]. We note that these systems have attracted some attention in the context of nano machines and thermoelectricity [162, 246]. It is also relevant to mention progress in quantum optoelectronics, by applying concepts of quantum optics to quantum electronics [247].

A specific example is based on the Anderson-Holstein Hamiltonian and circuit of Fig. 6 [148]

$$\hat{H} = \sum_{kl} \omega_k b_{kl}^\dagger b_{kl} + (a + a^\dagger) \sum_{kl} g_{kl} (b_{kl}^\dagger + b_{kl}) + \omega_0 a^\dagger a + g x (N-1) + H_{Anderson}. \tag{47}$$

Here, the sum l acts on the left and right transmission lines (not shown in Fig. 5 for simplicity) coupling to the cavity, and serving to transport the microwave signal and $H_{Anderson}$ describes the quantum dot. The capacitive coupling with the cavity g is assumed to be a capacitive coupling where N represents the dot occupancy and $x \propto (a + a^\dagger)$ the electric displacement field in the cavity. Following Refs. [144, 154], we can generalize the input-output theory for this situation and we obtain the transmission coefficient [148] :

$$t(\omega) = iJ(\omega)\chi_{xx}(\omega), \tag{48}$$

where $J(\omega)$ is of ohmic type and describe photon dissipation in the transmission lines and the (retarded) photon propagator $\chi_{xx}(t) = -i\theta(t)\langle[x(t), x(0)]\rangle$ can be evaluated using the Schwinger-Keldysh approach in certain limiting cases. At a general level, one can write χ_{xx} as :

$$\chi_{xx}(\omega) = \frac{\omega_0}{\omega^2 - \omega_0^2 - \omega_0 \Pi^R(\omega) + i\omega_0\kappa}; \tag{49}$$

the retarded function Π^R includes both the effects of frequency renormalization and damping due to the electronic environment, by analogy to the NMR situation, and $\kappa \sim 2\pi\alpha\omega_0$ describes dissipation in the photon field due to the small coupling with the transmission lines (photon wave-guides) [148]. Treating the coupling between light and matter (the quantum dot, here) to second order in perturbation, then we can establish again a connection with the Korringa-Shiba relation :

$$\Pi^R(t, t') = \Lambda_R(t, t') = -g^2 K(t - t'), \tag{50}$$

and $K(t - t')$ describes the charge fluctuations on the quantum dot similarly to Eq. (42). Let us first consider an exactly solvable non-interacting resonant level model with a width Γ (see Sec. 2) ; here, the resonant level width is given by a sum of the coupling parameters Γ_L and Γ_R in Fig. 5. Then, the Keldysh calculation can be done rigorously [148]. We choose the light frequency $\omega_0 \sim \Gamma$ (the analogue of the Kondo energy scale). The position of the level here is at the Fermi energy of the leads when $\mu_L = \mu_R = 0$ in Fig. 6. Other parameters regimes, in particular the low-frequency regime, have been studied in Ref. [149].

We study the effect of a large bias voltage V across the mesoscopic system, producing a non-linear $I - V$ characteristics across the quantum dot [186, 92, 93, 94]. Similar nonlinear effects have also been addressed in tunnel junctions coupled to a cavity [248]. For $1/eV \ll 1/\omega_0$, the electron motion becomes fast compared to the photon dynamics, and therefore we observe that the photon damping vanishes rapidly $\mathrm{Re}\,\Pi^R(\omega_0, V) \gg \mathrm{Im}\,\Pi^R(\omega_0, V)$ [148]. This implies that the phase associated with the transmitted signal converges to $\pi/2$. The origin of this phase $\pi/2$ here simply comes from the small dissipation limit (electrons are fast and the cavity is good). Note that such a phase $\pi/2$ implicitly assumes very small dissipation from the transmission lines carrying the AC signal.

In addition, one can build a precise analogy with a stochastic classical Langevin equation. In this large-bias regime, after integration of the matter (electrons in the mesoscopic system), one obtains an exact equation for the classical component of the cavity field in the Keldysh sense [148] :

$$\ddot{x}_c = -\omega_0 x_c - F(x_c) - \gamma(x_c)\dot{x}_c + \xi(t), \tag{51}$$

and $\langle\xi(t)\xi(t')\rangle = D(x_c)\delta(t - t')$ where the diffusion coefficient depends on the bias voltage. The force $F(x_c)$ can be obtained exactly for the resonant level situation on the dot, leading to an anharmonic potential. In this

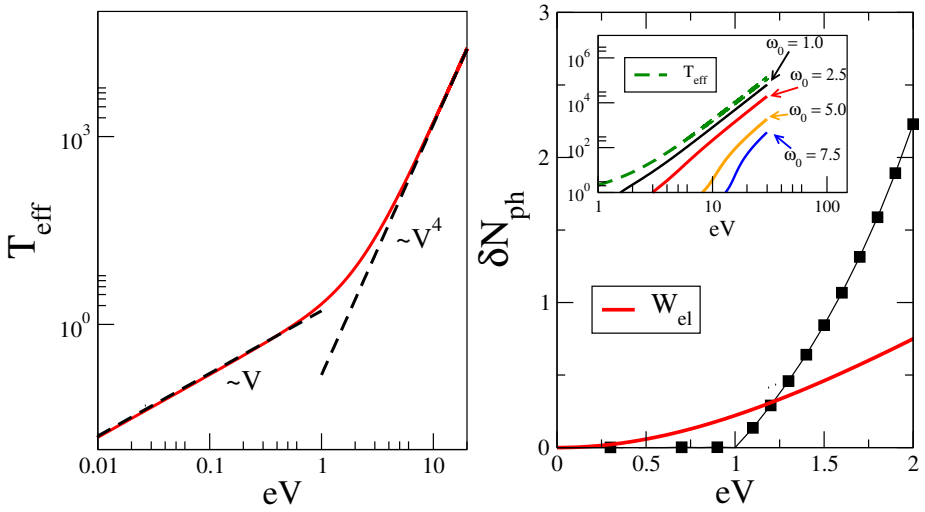

FIGURE 8 : Effective temperature T_{eff} for the cavity coupled to a resonant level model driven by a biased voltage V. Units are chosen such that $\omega_0 \sim \Gamma = 1$ and $g = 0.5\Gamma$. Mean Photon Number δN_{ph} or Effective Thermal Occupancy obtained with the Keldysh approach, and comparison with the dissipated power $W_{el} = I.V$ where I is the current flowing through the quantum dot system [148].

context, this analogy suggests an effective temperature $T_{eff} \sim D(V)/(4\gamma(V))$ in the cavity. By increasing the bias voltage across the mesoscopic system, we report a novel crossover in the light dynamics : at small bias voltages, the diffusion coefficient $D(V) \sim V$ and the friction coefficient γ is constant, leading to $T_{eff} \sim V$, whereas at large bias voltages compared to Γ, we report $T_{eff} \sim 1/\gamma \sim V^4$. In this limit, the motion of the electrons is fast enough such that the dissipation (friction) becomes negligible in agreement with the $\pi/2$ phase arguments above and the diffusion coefficient follows the current which saturates at large bias voltages [148]. It is also relevant to note that at this crossover, there is the production of a mean number of (thermal) photons in the cavity $\delta N_{ph} \sim T_{eff}/\omega_0 \sim V^4$ [148]. In Fig. 8, we draw the effective temperature as well as the induced (mean) photon number as a function of the bias voltage. In relation with the Korringa-Shiba relation, we note the following interesting property : at low frequency, we observe $\Lambda^R(\omega) = i\gamma(x_c)\omega$ even at large bias voltages [148]. We also note some connections with the Duffing oscillator model.

Let us now make a link to recent experiments in hybrid carbon systems, reporting some observation of Kondo physics with light measurements. The Kondo physics here refers to the formation of an entangled and Fermi liquid ground state between the effective spin in the mesoscopic system and electron reservoirs [213]. In Ref. [152], results in the spin Kondo regime of a carbon nanotube are consistent with a phase of the light signal following the DC conductance across the mesoscopic system in the low-frequency regime, in agreement with theory results (see Ref. [152] and Eq. (60) of Ref. [149]) based on admittance theory. Next, we describe a recent experiment in graphene double-dot quantum dot where the charge resonance condition described in Sec. 3.1 has also been achieved [153]. The experimental setup has been introduced and characterized in Refs. [249, 250]. A circuit-QED environment here couples to the left lead only, and by applying a gauge transformation we can reach a similar capacitive coupling as in Eq. (47) involving one of the two dots only [153]. The theory described above then can be adapted.

The reflection coefficient in the circuit-QED environment has been measured, by analogy to Eq. (37), and the resonance condition for light $(\omega_0^*(V))^2 = (\omega_0)^2 + \omega_0 \,\mathrm{Re}\,\Pi^R\left[\omega_0^*(V)\right]$ has been realized (these measurements are done at the light resonance condition). Datas shown in Ref. [153] seem consistent with an emergent Kondo fixed point, predicted by the theory in these double-dot charge qubits [251]. Again here, the effective spin corresponds to two macroscopic charge states on the mesoscopic system and the fixed point is assumed to exhibit an emergent $SU(4)$ symmetry as a result of entangled pseudo-spin (orbital-like) and spin degrees of freedom of conduction electron. The $SU(4)$ Kondo fixed point has also been studied experimentally in *GaAs* [252]. An analogy between a resonant level model and a Kondo low-energy fixed point can be formulated in the light of the emergent Fermi liquid ground state [253]. First, decoherence effects induced by the bias voltage produce a resonance width which

becomes bias dependent [254] :

$$\Gamma = T_K \text{ for } eV \ll T_K,$$
$$\Gamma \sim eV/\ln^2(eV/T_K) \text{ for } eV \gg T_K. \tag{52}$$

Here, T_K is the Kondo temperature scale (which is estimated around $550mK$ [153]). We have applied renormalization group arguments for the SU(4) Kondo effect, and obtained similar decoherence rates [153]. In addition, the $SU(4)$ symmetry moves the position of the effective resonance at an energy $\sim T_K$ [255]. By analogy with the photonic Kondo effect discussed in Sec. 3.1, the reflected microwave signal at the resonance condition for light $\omega = \omega_0^*$ again seems to reveal a phase shift of $2\delta(\omega_0^*) = \pi$, which is consistent with theoretical calculations [153]. Note that the DC phase shift is equal to $\delta(\omega = 0) = \pi/4$ for this $SU(4)$ Kondo fixed point [215, 253], due to the position of the Kondo resonance above the Fermi energy. These recent experiments [152, 153] are promising steps towards observing many-body features with light.

3.4. Spin-Boson Hamiltonians in Ladders : Quantum Microscope of Mott-Superfluid Transition, Artificial Gauge Fields and Chiral Currents

Now, we discuss engineering of the spin-boson model in ladder systems which may be realized in Josephson junction arrays, ultra-cold atoms and quantum circuits. The first realization of the spin-boson model in ultra-cold atoms has been proposed by Recati *et al.* [38] and generalized in Ref. [39]. A generalization to the context of mobile impurity has been addressed in Ref. [41]. Here, inspired by Ref. [181], we propose a slightly different version on a lattice where the spin-1/2 (a double well impurity) is used to probe the Mott-superfluid transition [168, 169, 170, 171] in a ladder system. This geometry also makes a connection with the Josephson-Kondo circuit of light, introduced in Sec. 3.1. We also note current efforts to address Kondo physics in ultra-cold atoms with fermionic environments [256].

We consider the system defined on the ladder geometry. At one extremity of the ladder we create a quantum microscope, a double-well system with occupancy one, as shown in Fig. 9(a). We suppose that interactions are sufficiently strong such that one realizes a state with one atom on the two wells (the two locations of the double well then correspond to the two polarization states of a spin-1/2 particle). The rest of the ladder forms the environment (bath). More precisely, we suppose that particles can hop to and from the impurity with the amplitude $t_{\parallel,s}$. We eliminate states with no occupancy on the microscope by fixing its chemical potential μ_s to be much bigger than the chemical potential of the bath μ_b, such that $\mu_s - \mu_b = \mu$, and we fix interaction terms U_s and $V_{\perp,s}$ large compared to the other energy scales of the system. Thus, single particle jumps to or from the impurity sites require high energy. We can then build second-order processes coupling the microscope with the ladder, and we obtain the Hamiltonian :

$$\hat{H} = \sum_q v|q| b^\dagger_{a,q} b_{a,q} + \frac{\sigma_z}{2} \sum_{q\neq 0} \lambda_q \left(b^\dagger_{a,q} + b_{a,-q} \right) + (nV_x + \Delta_0)\sigma_x \,, \quad \text{where}$$
$$\lambda_q = v \sqrt{\frac{\pi|q|}{L}} \left(\frac{aV_z}{2\pi v} \sqrt{K} - \frac{1}{\sqrt{K}} \right) . \tag{53}$$

By analogy to Sec. 3.1, only the anti-symmetric bosonic mode $b_{a,q}$ couples to the impurity. In addition, we suppose a direct tunnel coupling Δ_0 between the two wells. Here a is the spacing between lattice sites, L – the total length of the ladder, n – the filling of the bath, U – the strength of on-site Bose-Hubbard interactions, v – the speed of sound associated to the antisymmetric mode of the bath and K – the Luttinger parameter [34, 35]

$$v = a\sqrt{2nt_\parallel U} \,, \quad K = 2\pi \sqrt{\frac{nt_\parallel}{2U}} \,. \tag{54}$$

$t_\parallel$ and $t_{\parallel,s}$ are amplitudes of hopping between different sites in the bath and of the particle exchange between the

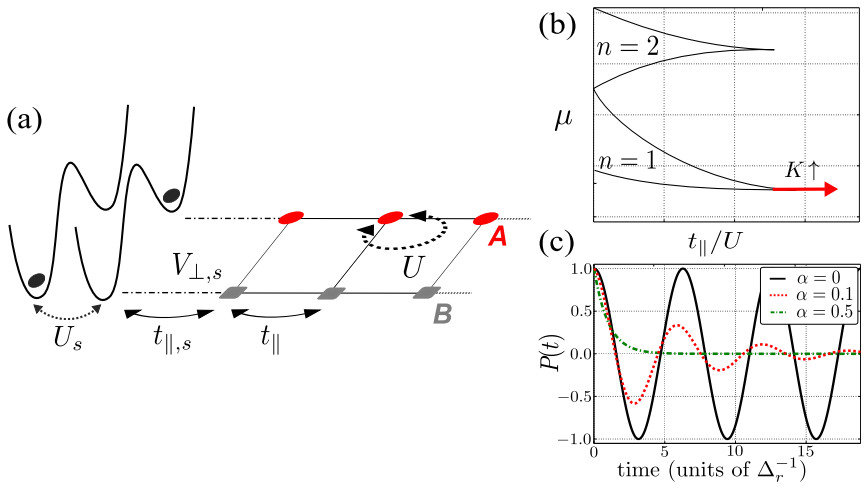

FIGURE 9 : **(a)** Model of the spin-impurity (quantum microscope) coupled to the low-energy excitations of the two-leg bosonic ladder. **(b)** Schematic representation of the Mott-Superfluid quantum phase transition of Berezinskii-Kosterlitz-Thouless type (for density $n=1$, the transition occurs at $t_\parallel/U \sim 0.3$ and $K=2$). Here, μ denotes the chemical potential in the ladder (μ_b in the text). **(c)** Relaxation of the spin-impurity initially polarized along the $\sigma_z=+1$ state for different values of the coherent coupling parameter (for completeness we show $P(t)=\langle\sigma_z(t)\rangle$ in relation with Fig. 2). We fix the chemical potential in the ladder in the vicinity of the tip of a Mott lobe in Fig. 9(b) which yields a cusp in one dimension, starting from the Mott phase (which does not exhibit sound modes ($\alpha=0$)), and consider increasing values of $t_\parallel$, such that the dissipation strength α in Eq. (57) increases in the BEC regime. The chemical potential in the impurity site is supposed to be higher to maintain an occupancy one on the double well system. Rabi oscillations of the impurity are related to the quantum tunneling between one well to the other, and sound modes of the BEC produces the dissipation in accordance with Sec. 2 and Eq. (11). In the text, the bare tunneling amplitude Δ can be obtained from Eq. (53).

spin and the bath respectively. Coupling amplitudes V_z and V_x are defined as follows :

$$V_z = -t_{\parallel,s}^2\left(\frac{1}{\mu+Un}-\frac{1}{V_{\perp,s}-\mu}+\frac{1}{U_s-\mu}\right),$$
$$V_x = -t_{\parallel,s}^2\left(\frac{1}{\mu+Un}-\frac{1}{V_{\perp,s}-\mu}\right). \tag{55}$$

We identify an ohmic spin-boson model. Since low-energy excitations in the ladder system are phonon-like only for wavelengths larger then the healing length $\xi = aK/n$, the high energy cut-off can be expressed as

$$\omega_c = v/\xi = nv/(aK)\ . \tag{56}$$

Finally, one can deduce the dimensionless dissipative parameter α

$$\alpha = \frac{1}{2K}\left(\frac{V_z}{2U}-1\right)^2 = \frac{1}{2K}\left[\frac{V_z}{t_\parallel n}\left(\frac{K}{2\pi}\right)^2-1\right]^2\ . \tag{57}$$

Dynamics of the spin is strongly related to the value of the dissipation parameter α. As an application, we discuss the evolution of the quantum microscope in time in the vicinity of the Mott-Superfluid transition, when fixing the mean density $n=1$ (this can be achieved by fixing the chemical potential in the ladder). In one dimension, such a transition is also of Berezinskii-Kosterlitz-Thouless type, then resulting in a cusp like profile in the phase diagram [35]. In the Mott regime $\alpha=0$: the Luttinger parameter of the bath is renormalized to zero and the spin is completely decoupled from the bath (see Fig. 9(b)). In this case we recover perfect Rabi oscillations of the microscope. If the bath moves away from the Mott regime, the dissipation parameter increases (the Luttinger parameter $K=2$ at the Mott-superfluid transition [257]) and the Rabi oscillations become underdamped for $\alpha<1/2$. When $\alpha=1/2$ the system would leave the coherent regime, in agreement with the arguments in Sec.

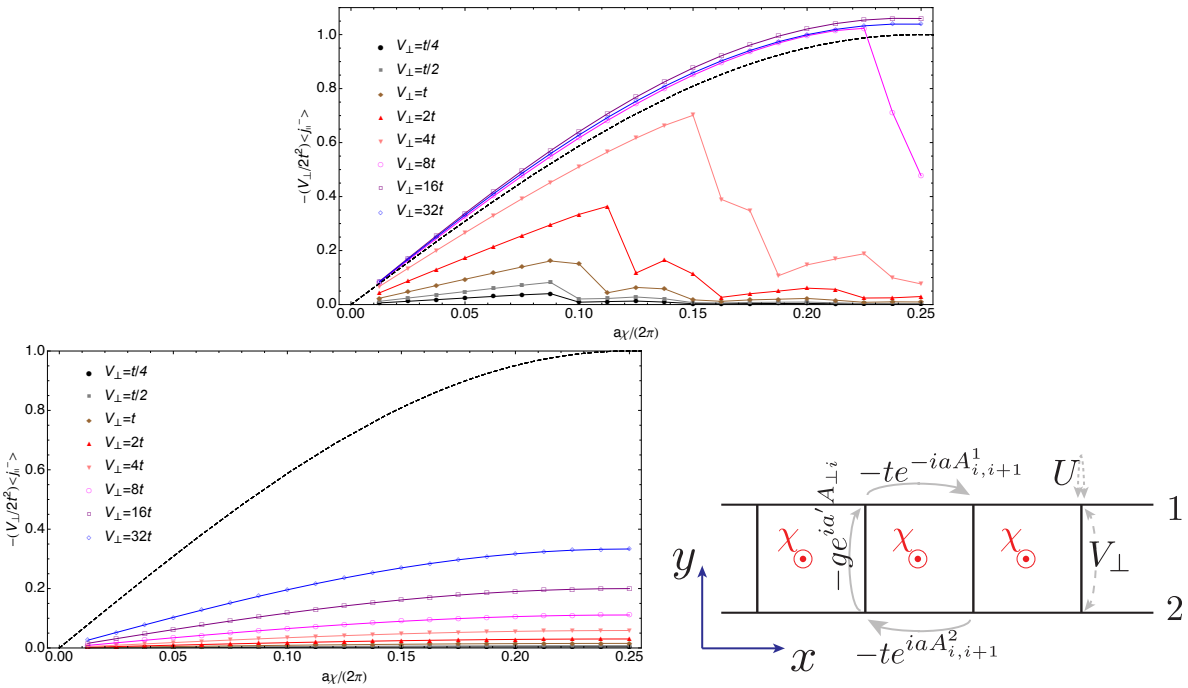

FIGURE 10 : DMRG Results for Meissner Currents in a Spin-Boson ladder, in a Mott phase with one boson per rung. The notations are fixed on the drawing of the ladder. The two figures are for a parallel hopping amplitude $t = 1$, in the hard-core boson limit ($U \to \infty$), and for Josephson couplings $g = 0.25$ (top) and $g = 32$ (bottom). For larger fluxes, we note that the details of the current amplitude depend on $V_\perp$ at smaller values of g (the ladder is relatively small here, with 24 rungs). The dashed black lines show the theoretical prediction $\langle j_\parallel \rangle = -2J_{xx}\sin(a\chi)$ with $J_{xx} = t^2/V_\perp$ valid for $V_\perp \gg t$ (in this figure, χ is the flux density). Decreasing $V_\perp$ increases the J_z coupling in the XXZ spin chain analogue (or XYZ spin chain with an equal coupling along X and Y direction) and the system approaches a spin density wave transition [177], suppressing the Meissner currents. We note that in general for finite size systems, even though the Meissner currents are still finite in the considered Mott phase, their amplitudes depend on the choice of parameters and size of the system.

2 (for rigorous figures obtained with the stochastic approach, see for example Fig. 2). The different regimes are shown in Fig. 9(c). It is important to mention the actual efforts both experimentally and numerically to localize the tip of Mott lobes in one dimension [258], which requires the development of concepts such as the bi-partite fluctuation measurements (see Ref. [259] and a comparison with various existing methods, and Refs. [260, 261, 262] for a review). We note recent experimental progress to measure such spin dynamics in ultra-cold atoms [263]. This could also be realized in cQED systems and Josephson junction arrays. The quantum microscope dynamics is also expected to measure novel glassy quantum dynamics induced by disorder [264, 265].

We also note that driven Floquet protocols on these type of spin-boson systems have been addressed recently theoretically [178]. In fact, similar spin impurity effects emerge in bosonic ladders, in relation with the Meissner and Josephson physics [266, 177]. The application of a uniform magnetic field produces currents which screen the applied magnetic field (resulting here in zero net current in a rung of a ladder). This property characterizes superconductors and superfluids. Recent experiments in cold atoms have succeeded in implementing such a Meissner effect in bosonic ladders using Floquet schemes to simulate artificial gauge fields [173]. Similar experiments in quantum transmon circuits have succeeded in building artificial gauge fields and quantum circulators in triangle geometries [182], following theoretical ideas [267, 268].

In such a two-leg ladder Bose-Hubbard model, the Josephson coupling between chains takes the form [177]

$$-g\cos(a'A_{\perp i} + \theta_{1i} - \theta_{2i}), \tag{58}$$

where θ_{1i} and θ_{2i} describe the superfluid phases in the two chains, a' is the distance between chains and $A_{\perp i}$ represents the vector potential induced by the uniform magnetic field in the direction of a rung (perpendicular to

the ladder) ; see Fig. 10. For strong Josephson couplings, the minimization of energy implies a zero net current on a given rung and the parallel current (density) flowing in the system from site i to j obeys $\langle j_{\parallel}\rangle = -2tn\text{phase}_{ij}$ at small applied magnetic flux per plaquette $a\chi \sim \text{phase}_{ij}$, where a is the lattice spacing in the horizontal direction ; here, we denote the tunneling amplitude along the chains $t_{\parallel} = t$. These Meissner currents have been observed both in ultra-cold atoms [173] and efforts to observe chiral currents in transmon cQED systems have been performed [182].

Interestingly, adding a strong inter-chain repulsion $V_{\perp}$ between the chains then one can stabilize a Mott state with one particle per rung [177]. Still, the system exhibits a 'spin' physics since on each rung, the particle can be in one of the two chains. In the limit of infinite on-site repulsion ($U \to \infty$), then one can build an equivalent spin model, where at each rung, we define spin operators $\sigma_x = b_1^{\dagger}b_2 + h.c$, $\sigma_y = -ib_1^{\dagger}b_2 + h.c$ and $\sigma_z = b_1^{\dagger}b_1 - b_2^{\dagger}b_2$. A similar construction has been used in transmon qubit systems [182]. The effective model in the Mott state, taking into account perturbative processes to second order, converges to the form of a solvable XXZ model subject to a transverse field [177]. The Josephson coupling turns into a spin magnetic field long the x direction and we find that the parallel Meissner currents are still non-zero in this Mott phase (because the gauge fields couple to the relative density or spin only), although there is a reduction compared to the superfluid phase : $\langle j_{\parallel}\rangle = -2J_{xx}\text{phase}_{ij}$ and $J_{xx} \sim t^2/V_{\perp}$ [177]. The theoretical prediction for $\langle j_{\parallel}\rangle$ is formally valid for large $V_{\perp}$ such that the J_z coupling of the effective XXZ spin chain is small enough. Decreasing $V_{\perp}$, then one can approach a spin density wave transition [177] suppressing the Meissner currents. Results obtained with the Density Matrix Renormalization Group (DMRG) approach with hard-core bosons ($U \to +\infty$) are shown in Fig. 10. The dashed black lines are the theoretical fits that should (only) be valid for infinite $V_{\perp}$ (a linear behavior of the current at small fluxes is found for all values of g). We also note that the Meissner currents tend to zero for small values of $V_{\perp}$ which tend to suggest that we reach a spin density wave transition.

We emphasize the numerous current efforts to realize novel correlated phases in these ladders systems with artificial gauge fields, related to flux phases [269, 270], vortex phases [271, 272, 273] and Laughlin phases [274, 275, 276]. We note the numerous theoretical proposals to realize exotic quantum Hall phases [277, 278, 279, 280, 281, 282, 283, 284, 285, 286, 287, 288, 289], in relation with wire-constructions of topological phases [290, 291, 292]. It is also important to mention novel efforts to predict and build Thouless pump type experiments [275, 276, 293, 294, 295].

4. Conclusion

In summary, we have addressed several points in relation with dissipative and driven many-body quantum systems. In particular, an environment can induce non-trivial dynamics at low temperatures producing entanglement, memory and decoherence. When studying the real time dynamics of spin observables, by analogy with classical Bloch equations, we have noted some analogy with a thermal state described by an effective temperature. At the same time, the stochastic dynamics of the quantum trajectories can produce novel phenomena in terms of many-body physics, such as localization and dissipation-induced quantum phase transitions, synchronization revivals, and a quantum dynamo effect when probing the topology of a driven spin-1/2 particle on the Bloch sphere. It is important to note that one is able to measure Berry phase properties of a spin-1/2 particle with the stochastic Schrödinger equation approach even though paths are encoded in classical blip and sojourn variables. Here, the Berry phase or Chern number is directly related to spin observables. Even at a mean-field level, studying quantum spin relaxation towards equilibrium in an Ising spin chain with long range forces can be complex in the presence of a non-Markovian environment. In the case of one-dimensional environments, one can also apply exact solutions through bosonization, Bethe Ansatz or direct approaches. Beyond studying these fundamental properties, an environment can also serve for bath (or dissipation) engineering. We have illustrated this point by studying Kondo physics of light in Josephson circuits in the microwave limit, emergent Kondo physics in quantum RC circuits, multi-channel Kondo fixed points in topological Josephson junctions with Majorana fermions, and hybrid systems comprising a cQED environment coupled to a biased mesoscopic system. A dissipative environment engenders fluctuations and disorder in time ; we have also analyzed this aspect by making connections between Kondo and Quantum Brownian motion physics. These quantum impurity systems can also be useful as sensors of quantum many-body phenomena and we have illustrated this aspect in ladder systems where the Rabi dynamics

of a spin-1/2 can probe the Mott-Superfluid transition. Ladder systems also build make a connection with the field of Floquet-induced exotic phases of matter and artificial gauge fields. These ladder systems are sufficiently simple to study important concepts such as realization of quantum Hall physics and topological physics, leading to the observation of protected chiral currents. At a more general level, we have also tried to unify several aspects of Floquet perturbations in relation with topology on the Bloch sphere, input signals in microwave circuits, AC perturbations in quantum RC circuits and the realization of artificial gauge fields to implement topological phases. Studying the fast dynamics in quantum materials has also attracted some attention recently, and we hope that our work could open new frontiers.

This work has been initiated by lectures given at Yale University, at Jouvence in Quebec and at CIFAR meetings, and at small classes at Ecole Polytechnique. We would like to dedicate this review to our dear friend and collaborator Adilet Imambekov whose original ideas initiated this work on the stochastic approach to the spin-boson model. The work on spin-boson and Kondo models have also been inspired from discussions with Markus Büttiker and Bernard Coqblin in Geneva, Sherbrooke and Paris. K.L.H. acknowledges support from the DOE DE-FG02-08ER46541, the German DFG Forschergruppe 2014, Ecole Polytechnique and Labex PALM. L. Henriet, L. Herviou, K. Plekhanov acknowledge support from Ecole Polytechnique and EDPIF Université Paris-Saclay. P.P.O. acknowledges support from Iowa State University Startup Funds.

Références

[1] P. Hänggi and G.L. Ingold, Fundamental Aspects of quantum Brownian motion, Chaos, vol. **15**, ARTN 026105 (2005).
[2] A. O. Caldeira and A.J. Leggett, Phys. Rev. Lett. **46** 211-214 (1981).
[3] J. Kondo, Prog. Theor. Phys. Oxford Journals. **32** (1) 37-49 (1964).
[4] P. W. Anderson, J. Phys. C : Solid St. Phys. **3** 2436-2441 (1970).
[5] K. Wilson, Rev. Mod. Phys. APS. **47** 773-840 (1975).
[6] Ph. Nozières, Jour. Low Temp. Phys. **17**, 31 (1974).
[7] M. Blume, V. J. Emery and A. Luther, Phys. Rev. Lett. **25** 450-453 (1970).
[8] A. J. Leggett, S. Chakravarty, A. T. Dorsey, M. P. A. Fisher, A. Garg and W. Zwerger, Rev. Mod. Phys, **59** 1 (1987).
[9] U. Weiss, Quantum dissipative systems, World Scientific, Singapore (2002).
[10] R. P. Feynman and F. L. Vernon, Ann. Phys. (N. Y.) **24**, 118 (1963).
[11] A. Georges, G. Kotliar, W. Krauth and M. Rozenberg Rev. of Mod. Physics. **68** 13-125 (1996).
[12] A. Tsvelick and P. Wiegmann, Advances in Physics, **32**, Issue 4, p.453-713 (1983).
[13] N. Andrei and H. Johannesson, **100** 108-112 (1984).
[14] K. Le Hur, Understanding Quantum Phase Transitions, edited by Lincoln D. Carr (Taylor and Francis, Boca Raton, 2010) and arXiv :0909.4822.
[15] S. F. Huelga, M. B. Plenio, Contemp. Phys. **54**, 181 - 207 (2013)
[16] C. Cohen-Tanoudji, J. Dupont-Roc and G. Grynberg, Photons and atoms, introduction to quantum electrodynamics, Wiley (1997)
[17] S. Haroche and J.-M. Raimond, Exploring the Quantum : Atoms, Cavities, and Photons, Oxford University Press (2006).
[18] R. J. Schoelkopf and S. M. Girvin, Wiring up quantum systems, Nature **451**, 664 (2008).
[19] A. A. Houck, H. Türeci and J. Koch, Nature Physics **8**, 292-299 (2012).
[20] S. Schmidt and J. Koch, Annalen der Physik, **525** 395-412 (2013).
[21] M. J. Hartmann, J. Opt. **18**, 104005 (2016).
[22] K. Le Hur, L. Henriet, A. Petrescu, K. Plekhanov, G. Roux and M. Schiro, C. R. Physique **17** 808-835 (2016).
[23] C. Noh and D. G. Angelakis, Report of Progress in Physics, **80** 016401 (2016).
[24] I. Carusotto and C. Ciuti, Rev. Mod. Phys. **85**, 299 (2013).
[25] I. Bloch, J. Dalibard and W. Zwerger, Rev. Mod. Phys. **80**, 885 (2008).
[26] F. Verstraete, M. M. Wolf and I. Cirac, Nature Physics **5**, 633 - 636 (2009).
[27] S. Diehl, A. Micheli, A. Kantian, B. Kraus, H. P. Büchler and P. Zoller, Nature Physics **4**, 878 -883 (2008).
[28] E. G. Dalla Torre, E. Demler, T. Giamarchi and E. Altman, Nat. Phys. **6**, 806-810 (2010).
[29] C.-E. Bardyn, M. A. Baranov, C. V. Kraus, E. Rico, A. Imamoglu, P. Zoller and S. Diehl, New Journal of Physics, **15**, Issue 8, 085001 (2013).
[30] F. Grusdt, N. Y. Yao, D. A. Abanin, M. Fleischhauer and E. A. Demler, Nature Communications **7**, 11994 (2016).
[31] E. Flurin, V. V. Ramasesh, S. Hacohen-Gourgy, L. S. Martin, N. Y. Yao and I. Siddiqi, arXiv :1610.03069.
[32] P. Cedraschi and M. Büttiker, Annals of Physics (NY) **289**, 1 - 23 (2001).
[33] K. Le Hur, Phys. Rev. Lett **92**, 196804 (2004).
[34] F. D. M. Haldane, J. Phys. C **14**, 2585 (1981).
[35] T. Giamarchi, Quantum Physics in One Dimension, Clarendon Press Oxford, 2004.
[36] I. M. Pop, I. Protopopov, F. Lecocq, Z. Peng, B. Pannetier, O. Buisson and W. Guichard, Nature Phys. **6**, 589 (2010).

[37] V. E. Manucharyan, J. Koch, L. Glazman and M. Devoret, Science **326**, 113-116 (2009).
[38] A. Recati, P. O. Fedichev, W. Zwerger, J. von Delft and P. Zoller, Phys. Rev. Lett. **94**, 040404 (2005).
[39] P. P. Orth and I. Stanic and K. Le Hur, Phys. Rev. A **77**, 051601(R) (2008).
[40] C. Sabin, A. White, L. Hackermuller and I. Fuentes, Nature Scientific Reports, Vol. **4**, id. 6436 (2014).
[41] A. Lamacraft, Phys. Rev. B **79**, 241105(R) (2009).
[42] O. Parlavecchio, C. Altimiras, J.-R. Souquet, P. Simon, I. Safi, P. Joyez, D. Vion, P. Roche, D. Esteve, and F. Portier, Phys. Rev. Lett., **114** (12) (2015).
[43] S. Jezouin, M. Albert, F. D. Parmentier, A. Anthore, U. Gennser, A. Cavanna, I. Safi and F. Pierre, Nat. Commun. **4** 1802 (2013).
[44] G.-L. Ingold and Yu. V. Nazarov, arXiv :cond-mat/0508728, in : Single Charge Tunneling, edited by H. Grabert and M. H. Devoret, NATO ASI Series B, Vol. 294, pp. 21-107 (Plenum Press, New York, 1992).
[45] C. L. Kane and M. P. A. Fisher, Phys. Rev. Lett. **68**, 1220 (1992).
[46] I. Safi and H. Saleur, Phys. Rev. Lett. **93** 126602 (2004).
[47] T. Giamarchi and H. J. Schulz, Phys. Rev. B **37**, 325 (1988).
[48] A. Kapitulnik, N. Mason, S. A. Kivelson and S. Chakravarty, Phys. Rev. B **63**, 125322 (2001).
[49] M. Fitzpatrick, N. M. Sundaresan, A. C. Y. Li, J. Koch, and A. A. Houck, arXiv :1607.06895.
[50] H. T. Mebrahtu, I. V. Borzenets, D. E. Liu, H. Zheng, Y. V. Bomze, A. I. Smirnov, H. U. Baranger and G. Finkelstein, Nature **488**, p. 61 (2012).
[51] P. Forn-Díaz, J. J. Garcia-Ripoll, B. Peropadre, M. A. Yurtalan, J.-L. Orgiazzi, R. Belyansky, C. M. Wilson, and A. Lupascu, arXiv :1602.00416.
[52] T. Goren, K. Le Hur, and E. Akkermans arXiv : arXiv :1611.06738.
[53] E. Akkermans and G. V. Dunne, Phys. Rev. Lett. **108**, 030401 (2012).
[54] M. Knap, A. Kantian, T. Giamarchi, I. Bloch, M. D. Lukin, and E. Demler, Phys. Rev. Lett. **111**, 147205 (2013).
[55] M. Atala, M. Aidelsburger, J. T. Barreiro, D. Abanin, T. Kitagawa, E. Demler, and I. Bloch, Nature Physics **9**, 795 (2013).
[56] M. Schiró and A. Mitra, Phys. Rev. Lett. **112**, 246401 (2014).
[57] M. Schiró and A. Mitra, Phys. Rev. B **91**, 235126 (2015).
[58] P. W. Anderson, G. Yuval, and D. R. Hamann, Phys. Rev. B **1** 4464-4473 (1970).
[59] H. Dekker, Phys. Rev. A, **35** 1436-1437 (1987).
[60] P. W. Anderson and G. Yuval, J. Phys. C **4**, 607-620 (1971).
[61] J. Zhang, P. W. Hess, A. Kyprianidis, P. Becker, A. Lee, J. Smith, G. Pagano, I.-D. Potirniche, A. C. Potter, A. Vishwanath, N. Y. Yao and C. Monroe, arXiv :1609.08684.
[62] S. Choi, J. Choi, R. Landig, G. Kucsko, H. Zhou, J. Isoya, F. Jelezko, S. Onoda, H. Sumiya, V. Khemani, C. von Keyserlingk, N. Y. Yao, E. Demler and M. D. Lukin, arXiv :1610.08057.
[63] D. J. Thouless, Phys. Rev. **187** 732-733 (1969).
[64] M-R. Li, K. Le Hur, and W. Hofstetter, Phys. Rev. Lett. **95**, 086406 (2005).
[65] G. Toulouse, C. R. Acad. Sci. **268**, 1200 (1969).
[66] F. Guinea, V. Hakim, and A. Muramatsu, Phys. Rev. B **32**, 4410 (1985).
[67] O. Kashuba, D. M. Kennes, M. Pletyukhov, V. Meden and H. Schoeller, Phys. Rev. B **88**, 165133 (2013).
[68] S. J. Weber, A. Chantasri, J. Dressel, A. N. Jordan, K. W. Murch and I. Siddiqi, Nature **511**, 570-573 (2014).
[69] N. Roch, M. E. Schwartz, F. Motzoi, C. Macklin, R. Vijay, A. W. Eddins, A. N. Korotkov, K. B. Whaley, M. Sarovar and I. Siddiqi, Phys. Rev. Letters, **112** (17), 170501 (2014).
[70] G. B. Lesovik, A. O. Lebedev, and A. O. Imambekov, JETP Lett. **75**, 474 (2002).
[71] J. Cao, L. W. Ungar, and G. A. Voth, J. Chem. Phys. **104**, 4189 (1996).
[72] W. T. Strunz, L. Diosi, and N. Gisin, Phys. Rev. Lett., **82**, 1801 (1999).
[73] J. T. Stockburger and C. H. Mac, J. Chem. Phys. **110**, 4983 (1999).
[74] J. T. Stockburger and H. Grabert, Phys. Rev. Lett. **88**, 170407 (2002).
[75] Y. Zhou and J. Shao, J. Chem. Phys. **128**, 034106 (2008).
[76] A. Imambekov, V. Gritsev, and E. Demler, in Proceedings of the 2006 Enrico Fermi Summer School on Ultracold Fermi gases, edited by M. Inguscio, W. Ketterle, and C. Salomon (Varenna, Italy, 2006).
[77] P. P. Orth, A. Imambekov and K. Le Hur Phys. Rev. A **82**, 032118 (2010) ; P. P. Orth, A. Imambekov, and K. Le Hur, Phys. Rev. B **87**, 014305 (2013).
[78] L. Henriet and K. Le Hur, Phys. Rev. B **93**, 064411 (2016).
[79] L. Henriet, Z. Ristivojevic, P. P. Orth, and K. Le Hur, Phys. Rev. A **90**, 023820 (2014).
[80] L. Henriet, A. Sclocchi, P. P. Orth and K. Le Hur, Phys. Rev. B **95**, 054307 (2017).
[81] Z. Ristivojevic, A. Petkovic, P. Le Doussal and T. Giamarchi, Phys. Rev. Lett. **109**, 026402 (2012).
[82] J. Dalibard, Y. Castin, and K. Molmer, Phys. Rev. Lett. **68**, 580 (1992).
[83] C. W. Gardiner, A. S. Parkins, and P. Zoller, Phys. Rev. A **46**, 4363 (1992).
[84] N. Gisin and I. C. Percival, J. Phys. A **25**, 5677 (1992).
[85] H.-P. Breuer, B. Kappler and F. Petruccione, Phys. Rev. A **59**, 1633 (1999).
[86] H. T. M. Nghiem and T. A. Costi, Phys. Rev. B **90**, 035129 (2014).
[87] M. Vojta, N.-H. Tong, and R. Bulla, Phys. Rev. Lett. **94**, 070604 (2005).
[88] F. B. Anders and A. Schiller, Phys. Rev. B **74**, 245113 (2006).
[89] K. Le Hur, Ph. Doucet-Beaupré, and W. Hofstetter, Phys. Rev. Lett. **99**, 126801 (2007).
[90] P. P. Orth, D. Roosen, W. Hofstetter and K. Le Hur, Phys. Rev. B **82**, 144423 (2010).
[91] A. Winter and H. Rieger, Phys. Rev. B **90**, 224401 (2014).
[92] M. Schirò and M. Fabrizio, Phys. Rev. B **79** 153302 (2009).
[93] T. L. Schmidt, P. Werner, L. Muehlbacher and A. Komnik, Phys. Rev. B **78**, 235110 (2008).

[94] P. Werner, T. Oka and A. J. Millis, Phys. Rev. B **79**, 035320 (2009).
[95] C. Xu, A. Poudel and M. G. Vavilov, Phys. Rev. A **89**, 052102 (2014).
[96] M. Bauer, D. Bernard and A. Tilloy, J. Stat. Mech. P09001 (2014).
[97] C. Schoen, K. Hammerer, M. M. Wolf, J. I. Cirac and E. Solano, Phys. Rev. A **75**, 032311 (2007).
[98] M. Marcuzzi, E. Levi, S. Diehl, J. P. Garrahan and I. Lesanovsky, Phys. Rev. Lett. **113**, 210401 (2014).
[99] M. L. Wall, A. Safavi-Naini and A. M. Rey, Phys. Rev. A **94**, 053637 (2016).
[100] J. Jin, A. Biella, O. Viyuela, L. Mazza, J. Keeling, R. Fazio and D. Rossini, Phys. Rev. X **6**, 031011 (2016).
[101] Z. Blunden-Codd, S. Bera, B. Bruognolo, N.-O. Linden, A. W. Chin, J. von Delft, A. Nazir and S. Florens, arXiv :1608.00799.
[102] P. Werner, K. Volker, M. Troyer, and S. Chakravarty, Phys. Rev. Lett. **94** , 047201 (2005).
[103] P. Werner, M. Troyer, and S. Sachdev, J. Phys. Soc. Jpn. Suppl. **74**, 67 (2005).
[104] S. Sachdev, P. Werner, M. Troyer, Phys. Rev. Lett. **92**, 237003 (2004).
[105] S. Pankov, S. Florens, A. Georges, G. Kotliar and S. Sachdev, Phys. Rev. B **69**, 054426 (2004).
[106] A. Georges, O. Parcollet and S. Sachdev, Phys. Rev. Lett., **85**, 840-843 (2000).
[107] H. Weber and M. Vojta, Eur. Phys. J. B **53**, 185 (2006).
[108] W. Wu, M. Ferrero, A. Georges and E. Kozik, arXiv :1608.08402.
[109] U. Bissbort, R. Thomale and W. Hofstetter, Phys. Rev. A **81**, 063643 (2010).
[110] G. Kulaitis, F. Krüger, F. Nissen and J. Keeling, Phys. Rev. A **87**, 013840 (2013).
[111] A. Le Boité, G. Orso and Cristiano Ciuti, Phys. Rev. Lett. **110** 233601 (2013).
[112] N. S. Williams, K. Le Hur, and A. N. Jordan, J. Phys. A : Math. Theor. **44** 385003 (2011).
[113] K. Le Hur, Ann. Phys. N.Y. **323** 2208-2240 (2008) and arXiv :0711.2301.
[114] A. Kopp and K. Le Hur, Phys. Rev. Lett. **98**, 220401 (2007).
[115] S. Braun, P. Ronzheimer, M. Schreiber, S. S. Hodgman, T. Rom, I. Bloch and U. Schneider, Science **339**, 52-55 (2013).
[116] A. Polkovnikov and V. Gritsev, PNAS **109**, 6457 (2012).
[117] M. V. Berry, Proceedings of the Royal Society A. **392** (1802) : 45Ð57 (1984).
[118] M. Kolodrubetz, P. Mehta and A. Polkovnikov, arXiv :1602.01062.
[119] M. Schroer, M. Kolodrubetz, W. Kindel, M. Sandberg, J. Gao, M. Vissers, D. Pappas, A. Polkovnikov, and K. Lehnert, Phys. Rev. Lett. **113**, 050402 (2014).
[120] P. Roushan, C. Neill, Y. Chen, M. Kolodrubetz, C. Quintana, N. Leung, M. Fang, R. Barends, B. Campbell, Z. Chen, B. Chiaro, A. Dunsworth, E. Jeffrey, J. Kelly, A. Megrant, J. Mutus, P. J. J. OMalley, D. Sank, A. Vainsencher, J. Wenner, T. White, A. Polkovnikov, A. N. Cleland, and J. M. Martinis, Nature **515**, 241-244 (2014).
[121] M. Aidelsburger, M. Lohse, C. Schweizer, M. Atala, J. T. Barreiro, S. Nascimbène, N. R. Cooper, I. Bloch, and N. Goldman, Nature Physics **11**, 162-166 (2015).
[122] N. Fläschner, B. S. Rem, M. Tarnowski, D. Vogel, D.-S. Lühmann, K. Sengstock, and C. Weitenberg, Science **352**, 1091 (2016).
[123] G. Jotzu, M. Messer, R. Desbuquois, M. Lebrat, T. Uehlinger, D. Greif, and T. Esslinger, Nature **515**, 237-240 (2014).
[124] N. Doiron-Leyraud, T. Szkopek, T. Pereg-Barnea, C. Proust and G. Gervais, Phys. Rev. B **91**, 245136 (2015).
[125] K. Bennaceur, J. Guillemette, P. L. Lévesque, N. Cottenye, F. Mahvash, N. Hemsworth, A. Kumar, Y. Murata, S. Heun, M. O. Goerbig, C. Proust, M. Siaj, R. Martel, G. Gervais and T. Szkopek, Phys. Rev. B **92**, 125410 (2015).
[126] Y. Zhang, Y.-W. Tan, H. L. Stormer and P. Kim, Nature **438**, 201-204 (2005).
[127] C. Emary and T. Brandes, Phys. Rev. E **67** 066203 (2003).
[128] O. Scarlatella and M. Schiró, arXiv :1611.09378.
[129] P. Strack and S. Sachdev, Phys. Rev. Lett. **107** 277202 (2011).
[130] G. Goldstein, C. Aron and C. Chamon, Phys. Rev. B **92**, 174418 (2015).
[131] P. Nalbach, S. Vishveshwara, and A. A. Clerk, Phys. Rev. B **92**, 014306 (2015).
[132] B. Neyenhuis, J. Smith, A. C. Lee, J. Zhang, P. Richerme, P. W. Hess, Z.-X. Gong, A. V. Gorshkov, and C. Monroe, arXiv :1608.00681.
[133] B. Yan, S. A. Moses, B. Gadway, J. P. Covey, K. R. A. Hazzard, A. Maria Rey, D. S. Jin and J. Ye, Nature **501** 521 (2013).
[134] R. Barends *et al.* Nature **534**, 222 (2016).
[135] O. Viehmann, J. von Delft and F. Marquardt, New J. Phys. **15**, 035013 (2013).
[136] L. Perfetti, B. Sciolla, G. Biroli, C. J. van der Beek, C. Piovera, M. Wolf and T. Kampfrath, Phys. Rev. Lett. **114**, 067003 (2015).
[137] Y. Liu, F. Piechon and J. N. Fuchs, Europhysics Letters **103**, 17007 (2013).
[138] M. Delehaye, S. Laurent, I. Ferrier-Barbut, S. Jin, F. Chevy, C. Salomon, arXiv :1510.06709 (2015).
[139] J. A. Acebrón, L. L. Bonilla, C. J. P. Vicente, F. Ritort, and R. Spigler Rev. Mod. Phys. **77**, 137 (2005).
[140] V. Flovik, F. Macia and E. Wahlström, Scientific Reports **6**, 32528 (2016).
[141] M. Sassetti and U. Weiss, Phys. Rev. Lett. **65**, 2262 (1990).
[142] H. Shiba, Prog. Theor. Phys. **54**, 967 (1975).
[143] M. Garst, P. Wölfle, L. Borda, J. von Delft and L. I. Glazman, Phys. Rev. B **72**, 205125 (2005).
[144] K. Le Hur, Phys. Rev. B **85**, 140506(R) (2012).
[145] M. Goldstein, M. H. Devoret, M. Houzet and L. I. Glazman, Phys. Rev. Lett. **110**, 017002 (2013).
[146] M. Büttiker, A. Prêtre and H. Thomas, Phys. Rev. Lett. **70**, 4114 (1993).
[147] C. Mora and K. Le Hur, Nature Physics **6**, 697 (2010).
[148] M. Schiró and K. Le Hur, Phys. Rev. B **89**, 195127 (2014).
[149] O. Dmytruk, M. Trif, C. Mora and P. Simon, Phys. Rev. B **93**, 075425 (2016).
[150] A. Cottet, T. Kontos and B. Douçot, Phys. Rev. B **91**, 205417 (2015).
[151] J. Gabelli, G. Fève, J.-M. Berroir and B. Plaçais, Rep. Prog. Phys. **75** 126504 (2012).
[152] M. R. Delbecq, V. Schmitt, F. D. Parmentier, N. Roch, J. J. Viennot, G. Fève, B. Huard, C. Mora, A. Cottet and T. Kontos, Phys. Rev. Lett. **107**, 256804 (2011).

[153] G.-W. Deng, L. Henriet, D. Wei, S.-X. Li, H.-O. Li, G. Cao, M. Xiao, G.-C. Guo, M. Schiro, K. Le Hur and G.-P. Guo, arXiv :1509.06141.
[154] A. Clerk, M.-H. Devoret, S. M. Girvin, F. Marquardt and R. Schoelkopf, Rev. Mod. Phys. **82**, 1155 (2010).
[155] H. Yi and C.L. Kane, Phys. Rev. B **57**, R5579 (1998) ; H. Yi, Phys. Rev. B **65**, 195101 (2002).
[156] P. Nozières and A. Blandin, J. Physique **41** 193 (1980)
[157] L. Herviou, K. Le Hur, and C. Mora, Phys. Rev. B (2016), Editor's Suggestion.
[158] K. Michaeli, L. Aviad Landau, E. Sela, L. Fu, arXiv :1608.00581.
[159] B. Beri and N. R. Cooper, Phys. Rev. Lett. **109**, 156803 (2012).
[160] A. Altland and R. Egger, Phys. Rev. Lett. **110**, 196401 (2013).
[161] E. Eriksson, C. Mora, A. Zazunov and R. Egger, Phys. Rev. Lett. **113**, 076404 (2014).
[162] B. Sothmann, R. Sánchez and A. N. Jordan, Nanotechnology **26**, 032001 (2015).
[163] R. M. Potok, I. G. Rau, H. Shtrikman, Y. Oreg and D. Goldhaber-Gordon, Nature, **446**, 7132, pp. 167-171 (2007) ; A. J. Keller, L. Peeters, C. P. Moca, I. Weymann, D. Mahalu, V. Umansky, G. Zaránd, D. Goldhaber-Gordon, Nature **526**, 237-240 (2015).
[164] Z. Iftikhar, S. Jezouin, A. Anthore, U. Gennser, F.D. Parmentier, A. Cavanna and F. Pierre, Nature **526**, 233 (2015).
[165] K. A. Matveev, Zh. Eksp. Teor. Fiz. **98**, 1598 (1990) [Sov. Phys. JETP **72**, 892 (1991)].
[166] K. A. Matveev, Phys. Rev. B **51**, 1743 (1995).
[167] Y. R. P. Sortais, H. Marion, C. Tuchendler, A. M. Lance, M. Lamare, P. Fournet, C. Armellin, R. Mercier, G. Messin, A. Browaeys and P. Grangier, Phys. Rev. A **75**, 013406 (2007).
[168] M. P. A. Fisher, G. Grinstein and D. S. Fisher, Physical Review B. **40** 546-70 (1989).
[169] D. Jaksch, C. Bruder, J. I. Cirac, C.W. Gardiner, and P. Zoller, Phys. Rev. Lett. **81**, 3108 (1998).
[170] M. Greiner, O. Mandel, T. Esslinger, T. W. Hänsch and I. Bloch, Nature **415**, 39-44 (2002).
[171] K. Le Hur and T. M. Rice, Annals of Physics **324**, 1452 (2009).
[172] M. Mancini, G. Pagano, G. Cappellini, L. Livi, M. Rider, J. Catani, C. Sias, P. Zoller, M. Inguscio, M. Dalmonte, and L. Fallani, ArXiv e-prints (2015), arXiv :1502.02495 [cond-mat.quant-gas].
[173] M. Atala, M. Aidelsburger, M. Lohse, J. T. Barreiro, B. Paredes and I. Bloch, Nature Physics **10**, 588-593 (2014).
[174] M. Lacki, H. Pichler, A. Sterdyniak, A. Lyras, V. E. Lembessis, O. Al-Dossary, J. C. Budich, and P. Zoller, Phys. Rev. A **93**, 013604 (2016).
[175] N. Goldman and J. Dalibard, Phys. Rev. X **4**, 031027 (2014).
[176] J. Cayssol, B. Dóra, F. Simon and R. Moessner, Phys. Status Solidi RRL **7** 101-108 (2013).
[177] A. Petrescu and K. Le Hur, Phys. Rev. B **91**, 054520 (2015).
[178] S. Restrepo, J. Cerrillo, V. M. Bastidas, D. G. Angelakis and T. Brandes, Phys. Rev. Lett. **117**, 250401 (2016).
[179] J. F. Sherson, C. Weitenberg, M. Endres, M. Cheneau, I. Bloch and S. Kuhr Nature **467**, 68 (2010).
[180] W. S. Bakr, J. I. Gillen, A. Peng, S. Fölling and M. Greiner, Nature **462**, 74-77 (2009).
[181] T. Fukuhara, A. Kantian, M. Endres, M. Cheneau, P. Schauss, S. Hild, D. Bellem, U. Schollwöck, T. Giamarchi, C. Gross, I. Bloch, S. Kuhr Nature Physics **9**, 235 (2013).
[182] P. Roushan *et al.* Nature Physics **13**, 146-151 (2017).
[183] S. Hershfield, Phys. Rev. Lett. **70**, 2134 (1993).
[184] P. Mehta and N. Andrei, Phys. Rev. Lett. **96**, 216802 (2006).
[185] B. Doyon, Phys. Rev. Lett. **99**, 076806 (2007).
[186] P. Dutt, J. Koch, J. E. Han and K. Le Hur, Annals of Physics **326** 2963-2999 (2011).
[187] L. Foini, L. F. Cugliandolo and A. Gambassi, J. Stat. Mech. (2012) P09011.
[188] L. Foini, A. Gambassi, R. Konik and L. F. Cugliandolo, arXiv :1610.00101.
[189] Cécile Monthus, arXiv :1701.05090.
[190] H. Li and F. D. M. Haldane, Phys. Rev. Lett. **101**, 010504 (2008).
[191] R. Thomale, A. Sterdyniak, N. Regnault and B. Andrei Bernevig, Phys. Rev. Lett. **104**, 180502 (2010).
[192] N. Lanatà, H. U. R. Strand, Y. Yao and G. Kotliar, Phys. Rev. Lett. **113**, 036402 (2014).
[193] R. Singh, J. H. Bardarson and F. Pollmann, New J. Phys. **18**, 023046 (2016).
[194] D. J. Luitz, N. Laflorencie and F. Alet, Phys. Rev. B **91**, 081103 (2015).
[195] R. Silbey, and R. A. Harris, J. Chem. Phys. **80**, 2615 (1984).
[196] D. P. S. McCutcheon, A. Nazir, S. Bose and A. J. Fisher, Phys. Rev. B **81**, 235321 (2010).
[197] R. S. Whitney and Y. Gefen, Phys. Rev. Lett. **90**, 190402 (2003).
[198] N. Flüschner, D. Vogel, M. Tarnowski, B. S. Rem, D.-Sören Lühmann, M. Heyl, J. C. Budich, L. Mathey, K. Sengstock and C. Weitenberg, arXiv :1608.05616.
[199] A. C. Hewson, The Kondo Problem to Heavy Fermions, Cambridge University Press 1997 ; B. Coqblin, Proceedings of the ARW Nato Workshop Hvar, Croatia (2002).
[200] S. F. Caballero-Benitez, G. Mazzucchi, I. B. Mekhov, Phys. Rev. A **93**, 063632 (2016).
[201] P. Nataf, M. Dogan and K. Le Hur, Phys. Rev. A **86**, 043807 (2012).
[202] R. A. Barankov and L. S. Levitov, Phys. Rev. Lett. **96**, 230403 (2006).
[203] Y. Makhlin, G. Schön and A. Shnirman, New Directions in Mesoscopic Physics (Towards Nanoscience), pp. 197-224. Eds. R. Fazio, V. F. Gantmakher, and Y. Imry, Kluwer, Dordrecht, 2003 ; arXiv :cond-mat/0309049.
[204] Y. A. Pashkin, T. Yamamoto, O. Astafiev, Y. Nakamura, D. V. Averin, and J. S. Tsai, Nature **421**, 823 (2003).
[205] W. G. van der Wiel, S. De Franceschi, J. M. Elzerman, T. Fujisawa, S. Tarucha and L.P. Kouwenhoven, Rev. Mod. Phys. Vol. **75** No. 1, 1-22 (2003).
[206] L. Borda, G. Zarand and P. Simon, Phys. Rev. B **72**, 155311 (2005).
[207] M. Haeberlein *et al.* arXiv :1506.09114.
[208] J. Koch *et al.* Phys. Rev. A **76**, 042319 (2007) ; A. A. Houck *et al.* Quant. Inf. Proc. **8**, 105 (2009).
[209] R. Barends *et al.* Phys. Rev. Lett.**111**, 080502 (2013).

[210] H. T. Mebrahtu, I. V. Borzenets, H. Zheng, Y. V. Bomze, A. I. Smirnov, S. Florens, H. U. Baranger and G. Finkelstein, Nature Physics **9**, 732 (2013)
[211] C.-H. Chung, K. Le Hur, G. Finkelstein, M. Vojta and P. Woelfle, Phys. Rev. B **87**, 245310 (2013).
[212] S. Camalet, P. Degiovanni, J. Schriefl and F. Delduc, Europhysics Letters **68** 37 (2004).
[213] L. I. Glazman and M. Pustilnik, New Directions in Mesoscopic Physics (Towards Nanoscience), eds. R. Fazio, V.F. Gantmakher, and Y. Imry (Kluwer, Dordrecht, 2003), pp. 93-115.
[214] T. A. Costi, Phys. Rev. Lett. **80**, 1038 (1998).
[215] I. Affleck, Acta Phys. Polon. B**26** 1869-1932 (1995).
[216] O. Astafiev, A. M. Zagoskin, A. A. Abdumalikov, Yu. A. Pashkin, T. Yamamoto, K. Inomata, Y. Nakamura, and J. S. Tsai, Science **327**, 840-843 (2010).
[217] B. Sbierski, M. Hanl, A. Weichselbaum, H. E. Türeci, M. Goldstein, L. I. Glazman, J. von Delft and A. Imamoglu, Phys. Rev. Lett. **111**, 157402 (2013).
[218] A. Leclair, F. Lesage, S. Lukyanov and H. Saleur, Phys. Lett. **A235** 203-208 (1997).
[219] J.-T. Shen and S. Fan, Phys. Rev. Lett. **98**, 153003 (2007).
[220] P. Longo, P. Schmitteckert and K. Busch, Phys. Rev. Lett. **104**, 023602 (2010).
[221] V. I. Yudson and P. Reineker, Phys. Rev. A **78**, 052713 (2008).
[222] M. Malekakhlagh, A. Petrescu and H. E. Türeci, Phys. Rev. A **94**, 063848 (2016).
[223] S. E. Nigg, R. Lopez and M. Büttiker, Phys. Rev. Lett. **97**, 206804 (2006).
[224] K. Le Hur and G. Seelig, Phys. Rev. B **65**, 165338 (2002).
[225] Y. Hamamoto, T. Jonckheere, T. Kato and T. Martin, Phys. Rev. B **81**, (2010) 153305.
[226] Y. Etzioni, B. Horovitz and P. Le Doussal, Phys. Rev. Lett. **106**, 166803 (2011).
[227] M. Filippone, K. Le Hur and C. Mora, Phys. Rev. Lett. **107**, 176601 (2011).
[228] M. Filippone, K. Le Hur and C. Mora, Phys. Rev. B **88**, 045302 (2013).
[229] P. Dutt, T. L. Schmidt, C. Mora and Karyn Le Hur, Phys. Rev. B **87**, 155134 (2013).
[230] M. Filippone and C. Mora Phys. Rev. B **86**, 125311 (2012).
[231] P. Coleman, L. Ioffe and A. M. Tsvelik, Phys. Rev. B **52**, 6611, (1995).
[232] C. Mora and K. Le Hur, Phys. Rev. B **88**, 241302 (2013).
[233] A. Golub and E. Grosfeld, Phys. Rev. B **86**, 241105(R) (2012).
[234] T. Müller, R. Thomale, B. Trauzettel, E. Bocquillon and O. Kashuba, arXiv :1701.03050.
[235] D. Litinski, P. W. Brouwer and M. Filippone, arXiv :1612.04822.
[236] Y. Oreg, G. Refael, and F. von Oppen, Phys. Rev. Lett. **105**, 177002 (2010).
[237] R. M. Lutchyn, J.D. Sau and S. Das Sarma, Phys. Rev. Lett. **105**, 077001 (2010).
[238] B. Béri, Phys. Rev. Lett. **110**, 216803 (2013).
[239] J. Dalibard, F. Gerbier, G. Juzeliünas and P. Öhberg, Rev. Mod. Phys. **83**, 1523 (2011).
[240] X.-Y. Feng, G.-M. Zhang and T. Xiang, Phys. Rev. Lett. **98**, 087204 (2007).
[241] T. A. Sedrakyan, L. I. Glazman and A. Kamenev, Phys. Rev. Lett. **114**, 037203 (2015).
[242] S. M. Albrecht, A. P. Higginbotham, M. Madsen, F. Kuemmeth, T. S. Jespersen, J. Nygard, P. Krogstrup, and C. M. Marcus, Nature **531**, 206 (2016).
[243] L. Aviad Landau and E. Sela, arXiv :1609.09257.
[244] A. Zazunov, F. Buccheri, P. Sodano and R. Egger, arXiv :1611.07307.
[245] J.J. Viennot, M.R. Delbecq, L.E. Bruhat, M.C. Dartiailh, M. Desjardins, M. Baillergeau, A. Cottet and T. Kontos, Comptes Rendus Physique **17** (7), 705-717 (2016).
[246] L. Henriet, A. N. Jordan and K. Le Hur, Phys. Rev. B **92**, 125306 (2015).
[247] E. Bocquillon, V. Freulon, F.D. Parmentier, J.-M Berroir, B. Plaçais, C. Wahl, J. Rech, T. Jonckheere, T. Martin, C. Grenier, D. Ferraro, P. Degiovanni and G. Fève, Annalen der Physik, **526**, 1 (2014).
[248] U. C. Mendes and C. Mora, Phys. Rev. B **93**, 235450 (2016).
[249] G.-W. Deng *et al.* Phys. Rev. Lett. **115**, 126804 (2015).
[250] G.-W. Deng *et al.* Nano Letters **15**, 6620 (2015).
[251] L. Borda, G. Zarand, W. Hofstetter, B. I. Halperin and J. von Delft, Phys. Rev. Lett. **90**, 026602 (2003).
[252] A. J. Keller *et al.* Nature Phys. **10** (2014) 145-150.
[253] C. Mora, P. Vitushinsky, X. Leyronas, A. A. Clerk and K. Le Hur, Phys. Rev. B **80**, 155322 (2009) (Editors' Suggestion).
[254] A. Rosch, J. Kroha and P. Wölfle, Phys. Rev. Lett. **87**, 156802 (2001).
[255] K. Le Hur, P. Simon and D. Loss, Phys. Rev. B **75**, 035332 (2007).
[256] J. Bauer, C. Salomon and E. Demler, Phys. Rev. Lett. **111**, 215304 (2013).
[257] T. Giamarchi and A. J. Millis, Phys. Rev. B **46**, 9325 (1992).
[258] G. Boéris, L. Gori, M. D. Hoogerland, A. Kumar, E. Lucioni, L. Tanzi, M. Inguscio, T. Giamarchi, C. D'Errico, G. Carleo, G. Modugno and L. Sanchez-Palencia, Phys. Rev. A **93**, 011601 (Rapid Comm.) (2016).
[259] S. Rachel, N. Laflorencie, H. Francis Song and K. Le Hur, Phys. Rev. Lett. **108**, 116401 (2012).
[260] H. F. Song, S. Rachel, C. Flindt, I. Klich, N. Laflorencie and K. Le Hur, Phys. Rev. B **85**, 035409 (2012), Editors' Suggestion.
[261] A. Petrescu, H. F. Song, S. Rachel, Z. Ristivojevic, C. Flindt, N. Laflorencie, I. Klich, N. Regnault and K. Le Hur, J. Stat. Mech. (2014) P10005.
[262] N. Laflorencie, Physics Report **643**, 1-59 (2016).
[263] B. Gadway, D. Pertot, J. Reeves, M. Vogt and D. Schneble, Phys. Rev. Lett. **107**, 145306 (2011).
[264] J. Billy, V. Josse, Z. Zuo, A. Bernard, B. Hambrecht, P. Lugan, D. Clément, L. Sanchez-Palencia, P. Bouyer, and A. Aspect, Nature **453**, Issue 7197, pp. 891-894 (2008).

[265] J.-y. Choi, S. Hild, J. Zeiher, P. Schauss, A. Rubio-Abadal, T. Yefsah, V. Khemani, D. A. Huse, I. Bloch and C. Gross, Science **352**, 1547 (2016).
[266] E. Orignac and T. Giamarchi, Phys. Rev. B **64** 144515 (2001).
[267] J. Koch, A. A. Houck, K. Le Hur, and S. M. Girvin, Phys. Rev. A **82**, 043811 (2010).
[268] A. Petrescu, A. A. Houck and K. Le Hur, Phys. Rev. A **86**, 053804 (2012).
[269] A. Dhar, M. Maji, T. Mishra, R. V. Pai, S. Mukerjee, and A. Paramekanti, Phys. Rev. A **85**, 041602 (2012) ; A. Dhar, T. Mishra, M. Maji, R. V. Pai, S. Mukerjee, and A. Paramekanti, Phys. Rev. B **87**, 174501 (2013).
[270] A. Tokuno and A. Georges, New J. Phys. **16**, 073005 (2014).
[271] M. Piraud, F. Heidrich-Meisner, I. P. McCulloch, S. Greschner, T. Vekua and U. Schollwoeck, Phys. Rev. B **91**, 140406(R), 2015.
[272] F. Kolley, M. Piraud, I. P. McCulloch, U. Schollwoeck and F. Heidrich-Meisner, New J. Phys. **17** 092001 (2015).
[273] E. Orignac, R. Citro, Mario Di Dio, S. De Palo and M.-L. Chiofalo, New Journal of Physics, **18** 055017 (2016).
[274] A. Petrescu and K. Le Hur, Phys. Rev. B **91**, 054520 (2015).
[275] A. Petrescu, M. Piraud, G. Roux, I. P. McCulloch, and K. Le Hur, arXiv :1612.05134.
[276] M. Calvanese Strinati, E. Cornfeld, D. Rossini, S. Barbarino, M. Dalmonte, R. Fazio, E. Sela and L. Mazza, arXiv :1612.06682.
[277] R. N. Palmer and D. Jaksch, Phys. Rev. Lett. **96**, 180407 (2003).
[278] A. S. Sorensen, E. Demler, and M. D. Lukin, Phys. Rev. Lett. **94**, 086803 (2005).
[279] M. Hafezi, A. S. Sorensen, E. Demler, and M. D. Lukin, Phys. Rev. A **76**, 023613 (2007).
[280] L. Hormozi, G. Moller and S. H. Simon, Phys. Rev. Lett. **108**, 256809 (2012).
[281] N. R. Cooper and J. Dalibard, Phys. Rev. Lett. **110**, 185301 (2013).
[282] N. Y. Yao, A. V. Gorshkov, C. R. Laumann, A. M. Läuchli, J. Ye and M. D. Lukin, Phys. Rev. Lett. **110**, 185302 (2013).
[283] A. Sterdyniak, B. A. Bernevig, N. R. Cooper, and N. Regnault, Phys. Rev. B **91**, 035115 (2015).
[284] M. Hafezi, M. D. Lukin, and J. M. Taylor, New Journal of Physics, **15**, 063001 (2013).
[285] E. Kapit, M. Hafezi, and S. H. Simon, Phys. Rev. X **4**, 031039 (2014).
[286] J. Cho, D. G. Angelakis, and S. Bose, Phys. Rev. Lett. **101**, 246809 (2008).
[287] A. L. C. Hayward, A. M. Martin, and A. D. Greentree, Phys. Rev. Lett. **108**, 223602 (2012).
[288] C. Noh and D. G. Angelakis, Reports on Progress in Physics **80**, 016401 (2017), arXiv :1604.04433 [quant-ph].
[289] B. M. Anderson, R. Ma, C. Owens, D. I. Schuster, and J. Simon Phys. Rev. X **6**, 041043 (2016).
[290] C. L. Kane, R. Mukhopadhyay, and T. C. Lubensky, Phys. Rev. Lett. **88**, 036401 (2002).
[291] J. C. Y. Teo and C. L. Kane, Phys. Rev. B **89**, 085101 (2014).
[292] T. Neupert, C. Chamon, C. Mudry and R. Thomale, Phys. Rev. B **90**, 205101 (2014).
[293] M. Lohse, C. Schweizer, O. Zilberberg, M. Aidelsburger and I. Bloch, Nature Phys. **12**, 350 (2016).
[294] S. Nakajima, T. Tomita, S. Taie, T. Ichinose, H. Ozawa, L. Wang, M. Troyer and Y. Takahashi, Nature Physics **12**, 296-300 (2016).
[295] J. Tangpanitanon, V. M. Bastidas, S. Al-Assam, P. Roushan, D. Jaksch and D. G. Angelakis, Phys. Rev. Lett. **117**, 213603 (2016).